

A general solution for accelerating screw dislocations in arbitrary slip systems with reflection symmetry

Daniel N. Blaschke

September 14, 2020

Los Alamos National Laboratory, Los Alamos, NM, 87545, USA

E-mail: dblaschke@lanl.gov

Abstract

Solutions to the differential equations of linear elasticity in the continuum limit in arbitrary crystal symmetry are known only for steady-state dislocations, i.e. line defects moving at constant velocity. Troubled by singularities at certain ‘critical’ velocities (typically close to certain sound speeds), these dislocation fields are thought to be too idealized, and divergences are usually attributed to neglecting the finite size of the core and to the restriction to constant velocity. In the isotropic limit, accelerating pure screw and edge dislocations were studied some time ago, but a generalization to anisotropic crystals has not been attempted before. This is the gap this work aims to fill, albeit restricted for now to pure screw dislocations and hence to slip systems featuring a reflection symmetry, a prerequisite to studying pure screw dislocations without mixing with edge dislocations. Further generalizations to include edge and mixed dislocations as well as regularizations of the dislocation core are beyond the scope of this paper and are left for future work.

Contents

1	Introduction and background	2
2	Solving the eom with Laplace and Fourier transforms	3
2.1	The general case	4
2.2	Constant velocity	12
2.3	Special case of constant acceleration	14
2.4	The isotropic limit	17
3	Conclusion	19
A	Rotation matrix and coefficients of the differential equation	19
B	Useful relations	21

1 Introduction and background

Plasticity in crystalline materials is governed by dislocations and at high stress and temperature their mobility becomes increasingly important, as it determines the glide time between obstacles (grain boundaries, impurities, other defects, etc.), thereby affecting Orowan's relation [1, 2]. Velocity v depends on dislocation drag B (the impediment of dislocation movement due to interaction with phonons, etc.) in a non-linear manner, and a reliable model of dislocation displacement gradient fields is a prerequisite for any model of $B(v)$ [3–6], an important ingredient of both discrete dislocation dynamics (DDD) simulations [7–10] and plasticity models [2, 11, 12]. Yet dislocation mobility in this regime is poorly understood, posing a major roadblock to further improving material strength predictions at high stress and temperature. A key question in this regard is whether dislocations can reach transonic and supersonic speeds under sufficiently high stress. Until some years ago it was believed that they cannot [13], based on the linear-elasticity derivation that the elastic self-energy of dislocations moving at constant velocity in the isotropic limit diverges at the transverse sound speed. However, in 2009 supersonic dislocations were observed in a plasma crystal [14]. Also, molecular dynamics (MD) simulations of screw and edge dislocations in some metals suggest that dislocation velocities can reach or even exceed the transverse wave speed [15–20]. Experiments cannot track dislocations in real time at these high speeds, but some crucial information is contained in measured stress versus strain rate curves. In particular, the highest measured strain rates (produced by overdriven shocks) are consistent with dislocations moving close to the lowest shear wave speed as a lower bound if, and only if, the density of mobile dislocations is comparable to the highest measured total dislocation density [12]. Despite positive MD results, clarifying whether supersonic dislocations exists in real metals will hence not only require a good understanding of the dislocation displacement gradient field itself, but will also require studying the dislocation density evolution; we will only focus on the dislocation field and not attempt the latter here.

Regarding dislocation theory, the displacement field of dislocations is determined by the equations of motion and the (leading order) stress-strain relations. Their solutions in the isotropic steady-state limit are well-known [13] and suffer from divergences at the transverse and longitudinal sound speed. See also [21] for a treatment of the subsonic, transonic, and supersonic regimes in the isotropic limit where each regime is separated from the others by a divergence in the dislocation field.

Solutions for accelerating screw and edge dislocations in the isotropic limit were derived by Markenscoff et al. [22–24], showing that an acceleration term together with a regularized dislocation core removes the divergence, thereby opening the possibility of supersonic events. An alternative treatment of the isotropic case which also emphasizes the need to account for size variations of the core can be found in a separate series of papers, Refs. [25–28].

Less is known in the more general anisotropic case, which is important because dislocation glide motion always happens within anisotropic single crystal grains (even in polycrystals): Solutions for the dislocation field for anisotropic crystals are known in the simple case of constant dislocation velocity [29]. A general method developed by Stroh and others [29] (and recently refined by Pellegrini [30]) can be used to derive solutions which suffer from diverging self-energies at the various wave speeds, suggesting that the lowest of those velocities is an upper bound. Ref. [31] also introduced a method to include an extended dislocation core with elliptic shape into this steady-state framework. For a recent nice review of dislocation dynamics, see Ref. [32].

The present work is a first step towards generalizing Markenscoffs results for accelerating dislocations to arbitrary anisotropic crystals. In particular, we study pure screw dislocations and, as a first step, neglect the dislocation core. This can only be done in slip systems exhibiting a reflection symmetry [33, Chapter 13], since only then do pure screw and edge dislocations decouple. All 12 fcc slip systems as well as a number of hcp slip systems share this property, though none of the 48 bcc slip systems do. As such, the results presented here are most useful to fcc crystals. It was recently pointed out that steady-state pure screw dislocations diverge at a ‘critical’ velocity that is different than any sound speed [20]. Here, we confirm for anisotropic crystals that (similar to the isotropic limit) this divergence is still present when acceleration is taken into account. Regularizing the dislocation core is hence required to eliminate the divergence entirely.

We also emphasize, that our present results represent the most general solution for accelerating pure screw dislocations in anisotropic crystals to date, which are interesting in their own right as well. In studying various limits, we recover many other known results, such as steady-state screw dislocations for subsonic and supersonic regimes and the isotropic limit.

2 Solving the eom with Laplace and Fourier transforms

The governing equations to which the displacement gradient field $u_{i,j} := \partial_j u_i$ provides a solution are the equations of motion and the (leading order) stress-strain relations known as Hooke’s law:

$$\begin{aligned} \partial_i \sigma_{ij} &= \rho \ddot{u}_j, & \sigma_{ij} &= C_{ijkl} \epsilon_{kl} = C_{ijkl} \partial_l u_k, \\ \epsilon_{kl} &:= (\partial_l u_k + \partial_k u_l)/2, \end{aligned} \tag{2.1}$$

where σ_{ij} denotes stress, ϵ_{kl} is the infinitesimal strain tensor (i.e. the symmetrized displacement gradient field), and ρ the material density.

For example, assuming cubic symmetry (e.g. fcc or bcc), the tensor of second order elastic constants within the crystal reference frame may be written as

$$C_{ijkl} = c_{12} \delta_{ij} \delta_{kl} + c_{44} (\delta_{ik} \delta_{jl} + \delta_{il} \delta_{jk}) - (2c_{44} + c_{12} - c_{11}) \sum_{\alpha=1}^3 \delta_{i\alpha} \delta_{j\alpha} \delta_{k\alpha} \delta_{l\alpha}, \tag{2.2}$$

where the first two terms are invariant under rotations. The last term explicitly depends on the crystal basis vectors, which in the present (Cartesian) case coincide with $\hat{x}_i = \delta_i^1$, $\hat{y}_i = \delta_i^2$, and $\hat{z}_i = \delta_i^3$, and as such it must be transformed into the coordinate basis one wishes to perform calculations in.

2.1 The general case

For some slip system geometries (but not all), pure screw and edge dislocations can be treated separately. This is only possible if a pure screw component gives rise *only* to displacements u_z in coordinates where \hat{z} is aligned with the dislocation line sense (and equally an edge component gives rise only to displacements u_x and u_y). As discussed in Ref. [33, Chapter 13], this is the case for slip systems where the x, y plane (in coordinates aligned with the dislocation) is a reflection plane, since only then does $u_x = 0 = u_y$ imply the vanishing of stresses in the $x-y$ plane, i.e. $\sigma_{xx} = \sigma_{yy} = \sigma_{xy} = 0$. For example, in cubic crystals this condition is fulfilled for all 12 fcc slip systems, but not for any bcc slip systems. Additionally, a number of hcp slip systems also fulfill the symmetry requirements of the present derivation.

The differential equation (2.1) was written in terms of Cartesian coordinates aligned with the (cubic) crystal axes. Solving it for a pure screw dislocation is however more conveniently carried out in coordinates aligned with the dislocation. Hence, we presently choose our coordinate system with \hat{z} aligned with the dislocation line and \hat{y} with the slip plane normal. By definition, the Burgers vector is aligned with the dislocation line sense of a pure screw dislocation, and provided the symmetry requirements described above are fulfilled for a slip system of interest, the displacement vector for pure screw dislocations will take the form $\vec{u} = (0, 0, u_z(x, y, t))$. Assuming the dislocation is much longer than a Burgers vector, the only velocity component that matters for dislocation glide is then normal to the dislocation line and therefore parallel to \hat{x} . In the rotated coordinate frame, the differential equation for a pure screw dislocation reads

$$\rho \partial_t^2 u_z(x, y, t) = (A \partial_x^2 + B \partial_x \partial_y + C \partial_y^2) u_z(x, y, t), \quad (2.3)$$

where numerical coefficients A , B , and C are functions of the second order elastic constants (c_{11} , c_{12} , and c_{44} in the case of cubic symmetry) as well as the rotation matrix that transforms between the crystal coordinates and our present coordinates which in turn depend on the slip system geometry. Coefficients A , B , and C for the fcc slip systems were previously presented in Ref. [20] in the context of the steady-state limit of Eq. (2.3). For completeness, we derive these coefficients once more in Appendix A.

The boundary conditions appropriate for a screw dislocation with Burgers vector $b\hat{z}$ are

$$u_z(x, y \rightarrow 0^\pm, t) = \pm \frac{b}{2} \Theta(x - l(t)), \quad \sigma_{yy}(x, 0, t) = 0 \quad \forall t > 0, \quad (2.4)$$

where $\Theta(x)$ denotes the Heaviside step function. The second condition encodes the requirement that no external concentrated force need to be applied in the y -direction at the core of the dislocation, and it is automatically fulfilled by a pure screw dislocation since $u_y = 0$. The first boundary condition encodes the discontinuity upon crossing the slip plane from negative to positive y , i.e. the displacement changes sign when approaching $y \rightarrow 0$ from above or below the slip plane.

The static case is included by these boundary conditions upon setting $l(t) = 0$ and $u_z(x, y, t) = u_z(x, y, 0)$. In the general case with $l(t) \neq 0$, it is convenient to employ a Laplace transform in time t and a Fourier transform (or two-sided Laplace transform which is related to the former) in one spatial variable, and it is convenient to transform x in this case due to the boundary condition (2.4). In particular:

$$\mathcal{L}\{u\} = \int_0^\infty u e^{-st} dt, \quad \mathcal{F}\{u\} = \frac{1}{\sqrt{2\pi}} \int_{-\infty}^\infty u e^{ikx} dx, \quad (2.5)$$

and it will be convenient to write the Fourier transform of u as a function of $\alpha := k/s$. Furthermore, we will make use of the Cagniard-de Hoop method [34–37] whose strategy it is to perform the

integration of the *inverse* Fourier transform along such a path that the resulting integral can be recognized as the Laplace transform of a certain function of time¹. Applying both transforms (2.5) to the differential equation (2.3) after dividing by A , we find

$$\begin{aligned} 0 &= \frac{1}{\sqrt{2\pi}} \int_{-\infty}^{\infty} dx \int_0^{\infty} dt e^{-st+isax} \left[\frac{s^2}{c_A^2} + s^2 \alpha^2 + i\tilde{B}s\alpha\partial_y - \tilde{C}\partial_y^2 \right] u_z(x, y, t) \\ &= \left[s^2 \left(\alpha^2 + \frac{1}{c_A^2} \right) + i\tilde{B}s\alpha\partial_y - \tilde{C}\partial_y^2 \right] \mathcal{F}\{\mathcal{L}\{u_z\}\}(\alpha, y, s), \end{aligned} \quad (2.6)$$

where $c_A = \sqrt{A/\rho}$, $\tilde{C} = C/A$, and $\tilde{B} = B/A$. Using the method of split variables and requiring the solution be bounded as $y \rightarrow \pm\infty$, we deduce

$$\mathcal{F}\{\mathcal{L}\{u_z\}\}(\alpha, y, s) = U(\alpha, s) e^{-s\tilde{\beta}y}, \quad (2.7)$$

with $\text{sgn}(y)\Re(\tilde{\beta}) > 0$. We find

$$\tilde{C}\tilde{\beta}^2 + i\tilde{B}\alpha\tilde{\beta} - \left(\alpha^2 + \frac{1}{c_A^2} \right) = 0,$$

and hence

$$\begin{aligned} \tilde{\beta} &= \frac{1}{2\tilde{C}} \left(-i\tilde{B}\alpha + \text{sgn}(y) \sqrt{4\tilde{C} \left(\alpha^2 + \frac{1}{c_A^2} \right) - \tilde{B}^2 \alpha^2} \right) \\ &= \text{sgn}(y) \sqrt{\frac{\alpha^2}{\tilde{C}} \left(1 - \frac{\tilde{B}^2}{4\tilde{C}} \right) + \frac{1}{c_A^2 \tilde{C}}} - i \frac{\tilde{B}\alpha}{2\tilde{C}}. \end{aligned} \quad (2.8)$$

Assuming that $\tilde{B}^2 < 4\tilde{C}$, we must choose the sign of the square root according to $\text{sgn}(y)$ and hence find that

$$\tilde{\beta}y = \beta|y|, \quad \beta = \left(\sqrt{\frac{1}{c_A^2 \tilde{C}} - \frac{p^2}{\tilde{C}} \left(1 - \frac{\tilde{B}^2}{4\tilde{C}} \right)} - \text{sgn}(y) \frac{\tilde{B}p}{2\tilde{C}} \right), \quad (2.9)$$

with $p = i\alpha = ik/s$ being a further variable substitution whose purpose will become clear below. In Appendix A we check explicitly that the condition $\tilde{B}^2 < 4\tilde{C}$ is indeed fulfilled for all 12 fcc slip systems, and one may check that this also the case for a number of hcp slip systems with reflection symmetry.

Making use of our boundary conditions, we determine $U(\alpha, s)$ as follows:

$$\begin{aligned} U(\alpha, s) &= \mathcal{F}\{\mathcal{L}\{u_z(x, 0^\pm, t)\}\} = \frac{\pm 1}{\sqrt{2\pi}} \int_{-\infty}^{\infty} dx \int_0^{\infty} dt e^{-st+isax} \frac{b}{2} \Theta(x - l(t)) \\ &= \pm \frac{b}{2\sqrt{2\pi}} \int_0^{\infty} dx \int_0^{\eta(x)} dt e^{-st+isax} \\ &= \frac{\pm b}{2\sqrt{2\pi}} \int_0^{\infty} dx e^{isax} \frac{1}{s} \left(1 - e^{-s\eta(x)} \right), \end{aligned} \quad (2.10)$$

¹ The same methods have also been applied to the theory of seismic faults which can be described in terms of isotropic dislocations, see e.g. [38–41] and references therein. I thank B. Gurrutxaga-Lerma for pointing me to these references.

where $\eta(x) := l^{-1}(x)$ is strictly positive since the integral is over $t > 0$, and (without loss of generality) we consider $l(t)$ to be a monotonically growing function of t . For non-vanishing y , the correct sign is encoded by $\text{sgn}(y)$. The next step is to apply the inverse Fourier transform; we presently have

$$\begin{aligned}\mathcal{L}\{u\}(x, y, s) &= \frac{1}{\sqrt{2\pi}} \int_{-\infty}^{\infty} dk e^{-ikx} U(\alpha = k/s, s) e^{-s\beta|y|} \\ &= \frac{b \text{sgn}(y)}{4\pi} \int_{-\infty}^{\infty} dk e^{-ikx} \int_0^{\infty} dx' e^{ikx'} \frac{1}{s} (1 - e^{-s\eta(x')}) e^{-s\beta|y|}.\end{aligned}\quad (2.11)$$

The integral over x' can be solved analytically only for simple special cases of $\eta(x')$, like for example for a dislocation initially at rest and then ‘suddenly’ moving at constant velocity v from time $t > 0$ leading to $\eta(x') \rightarrow x'/v$ (with x' positive). We will for now keep $\eta(x')$ general which requires us to exchange the two integrals in the second term and to solve for the integral over dp first there. This is permissible only if both integrals converge absolutely, but in the expression above this is not the case as discussed in Ref. [37] (for the isotropic limit), and as we will also see below. In fact, solving for $\mathcal{L}\{u\}(x, y, s)$ directly is troublesome due to subtleties with regard to poles, and instead we proceed to solve for its gradient, i.e.:

$$\begin{aligned}\partial_x \mathcal{L}\{u\}(x, y, s) &= \frac{-ib \text{sgn}(y)}{4\pi} \left[\int_{-i\infty}^{i\infty} dp e^{-spx} e^{-s\beta|y|} + \int_{-i\infty}^{i\infty} dp e^{-spx} \int_0^{\infty} dx' e^{spx'} s p e^{-s\eta(x')} e^{-s\beta|y|} \right], \\ \partial_y \mathcal{L}\{u\}(x, y, s) &= \frac{-ib}{4\pi} \left[\int_{-i\infty}^{i\infty} dp e^{-spx} e^{-s\beta|y|} \lim_{\epsilon \rightarrow 0^+} \left(\frac{s\beta}{sp - \epsilon} \right) + \int_{-i\infty}^{i\infty} dp e^{-spx} \int_0^{\infty} dx' e^{spx'} s \beta e^{-s\eta(x')} e^{-s\beta|y|} \right],\end{aligned}\quad (2.12)$$

where the variable substitution $k = -ips$ and $dk = -isd p$ was employed. Following the Cagniard-Hoop method [34, 35, 37], we wish to find a further variable substitution that allows us to rewrite the integral over the purely imaginary variable p in terms of a strictly positive variable τ such that the integrand in terms of τ is recognized as a Laplace transform of a certain function of time. This can be done via complex analysis by identifying an appropriate closed path in complex space over which to integrate and by using Cauchy’s theorem stating that the integral over such a closed path equals the residua of any poles enclosed by that path.

In the isotropic limit, it was shown in Ref. [37], that after exchanging the integrals, the remaining integral over x' exhibits a quadratic pole in its integrand at $x' \rightarrow x$ if $y = 0$ and $x \geq 0$ and converges otherwise. We will see below in Eq. (2.26) that this is also the case in the present anisotropic generalization, and in order to remove this (and a subleading) pole we add and subtract a term with $\eta(x')$ replaced by its linear order Taylor series expansion² $\tilde{\eta} = \eta(x) + (x' - x)\eta'(x)$ where we define $\eta'(x) := \text{sgn}(x)\partial_x \eta(|x|) \geq 0$ and $\eta(x) := \text{sgn}(x)\eta(|x|)$. By changing the overall sign of $\tilde{\eta}$ according to the sign of x (and we have this freedom as there is no pole for $x < 0$), we ensure that the two x' integrals cancel one another in the special case of constant velocity (see Section 2.2 below), thereby significantly simplifying that special case.

²Note that the term to be added and subtracted in Ref. [37, Eq. (24)] has the wrong dimensions and is clearly missing a factor $\beta e^{(-s\lambda\xi)}$ where the notation in that paper corresponds to ours via $\lambda = p$ and $\xi = x'$; otherwise the general strategy of removing the pole is the same as ours. We also point out that the importance of adding and subtracting such terms was not emphasized in some later papers by the same author [22, 23], and this may lead to the impression that the isotropic solution is highly singular at $y = 0$; see e.g. an according comment in [26]. In fact, as we see in our present derivation, the solution is well-behaved if appropriate terms are added and subtracted for all values of y prior to exchanging the order of integration.

Because of its linear dependence on x' in the exponent, the x' integral can be performed exactly and without exchanging the integral order in the added term. In the subtracted term, the integral order is exchanged in order to remove the pole. In particular, we consider

$$\begin{aligned}
\partial_x \mathcal{L}\{u\}(x, y, s) &= \frac{-ib \operatorname{sgn}(y)}{4\pi} \left[\int_{-i\infty}^{i\infty} dp e^{-spx} e^{-s\beta|y|} + \int_{-i\infty}^{i\infty} dp e^{-spx} \int_0^\infty dx' e^{spx'} s p e^{-s\tilde{\eta}} e^{-s\beta|y|} \right. \\
&\quad \left. + \int_0^\infty dx' \left(e^{-s\eta(x')} - e^{-s\tilde{\eta}} \right) \int_{-i\infty}^{i\infty} dp e^{-sp(x-x')} e^{-s\beta|y|} s p \right] \\
&= \frac{-ib \operatorname{sgn}(y)}{4\pi} \left[\int_{-i\infty}^{i\infty} dp e^{-spx} e^{-s\beta|y|} + e^{-s(\eta(x)-x\eta'(x))} \int_{-i\infty}^{i\infty} dp e^{-spx} e^{-s\beta|y|} \frac{p}{\eta'(x)-p} \right. \\
&\quad \left. + \int_0^\infty dx' \left(e^{-s\eta(x')} - e^{-s\tilde{\eta}} \right) s \int_{-i\infty}^{i\infty} dp e^{-sp(x-x')} e^{-s\beta|y|} p \right], \tag{2.13a}
\end{aligned}$$

$$\begin{aligned}
\partial_y \mathcal{L}\{u\}(x, y, s) &= \frac{-ib}{4\pi} \left[\int_{-i\infty}^{i\infty} dp e^{-spx} e^{-s\beta|y|} \lim_{\epsilon \rightarrow 0^+} \left(\frac{s\beta}{sp-\epsilon} \right) + e^{-s(\eta(x)-x\eta'(x))} \int_{-i\infty}^{i\infty} dp e^{-spx} e^{-s\beta|y|} \frac{\beta}{\eta'(x)-p} \right. \\
&\quad \left. + \int_0^\infty dx' \left(e^{-s\eta(x')} - e^{-s\tilde{\eta}} \right) s \int_{-i\infty}^{i\infty} dp e^{-sp(x-x')} e^{-s\beta|y|} \beta \right], \tag{2.13b}
\end{aligned}$$

where exchanging the order of integration is now allowed after having subtracted the poles under the x' integral.

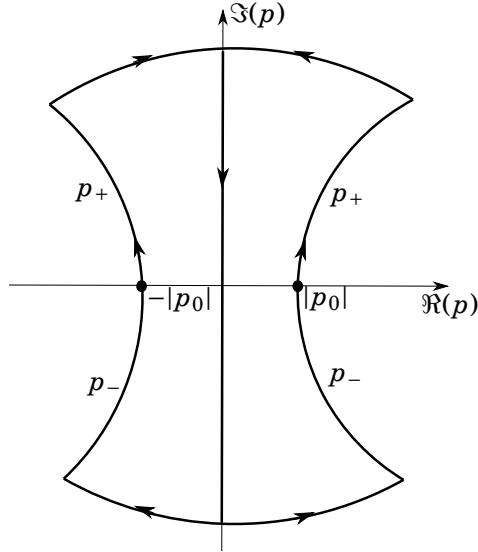


Figure 1: We illustrate the path of integration in the complex p -plane: The initial integral over the imaginary axis of p is closed via $p_{\pm}(\tau)$ which are connected to the imaginary axis at $\Im(p) = \pm\infty$. The real axis is crossed at $p_0 = p(\tau_{\min})$ and its sign is given by the sign of $x - y \frac{\tilde{B}}{2C}$.

Choosing the path:

The final step is to choose appropriate paths for the integrals over p , so that the integrals are rewritten in a way that can be identified as Laplace transforms in time. In other words, we need

$$\begin{aligned}(\beta|y| + px) &\equiv \tau > 0, & \tau \in \mathfrak{R}, \\(\beta|y| + p(x - x')) &\equiv \tau' > 0, & \tau' \in \mathfrak{R},\end{aligned}\tag{2.14}$$

and τ (resp. τ') are subsequently interpreted as a time variable within a Laplace transform. We proceed by deriving $p(\tau)$ and note that $p(\tau')$ follows trivially by shifting $x \rightarrow (x - x')$. The definition above together with (2.9) leads to a quadratic equation in p , namely

$$p^2 \left(x^2 - xy \frac{\tilde{B}}{\tilde{C}} + \frac{y^2}{\tilde{C}} \right) - p\tau \left(2x - y \frac{\tilde{B}}{\tilde{C}} \right) + \tau^2 - \frac{y^2}{c_A^2 \tilde{C}} = 0,\tag{2.15}$$

with solutions

$$p_{\pm} = \frac{1}{R^2} \left(\tau \left(x - y \frac{\tilde{B}}{2\tilde{C}} \right) \pm i|y| \sqrt{\tau^2 \frac{1}{\tilde{C}} \left(1 - \frac{\tilde{B}^2}{4\tilde{C}} \right) - \frac{R^2}{c_A^2 \tilde{C}}} \right),\tag{2.16}$$

where $R^2 = \left(x^2 - xy \frac{\tilde{B}}{\tilde{C}} + \frac{y^2}{\tilde{C}} \right)$. The square root within p_{\pm} is real for $\tau > \tau_{\min} = R / \left(c_A \sqrt{1 - \tilde{B}^2/4\tilde{C}} \right) \geq 0$ since we already established that $1 - \tilde{B}^2/4\tilde{C} > 0$. From the expression (2.16), we see that $\tau \in [\tau_{\min}, \infty)$ yields hyperbolas in the complex plane of p_{\pm} , as illustrated in Figure 1. The real axis is crossed at $p_0 := p_{\pm}(\tau_{\min})$ with

$$|p_0| = |p_{\pm}(\tau_{\min})| = \frac{\left| x - y \frac{\tilde{B}}{2\tilde{C}} \right|}{R c_A \sqrt{1 - \frac{\tilde{B}^2}{4\tilde{C}}}} = \frac{\sqrt{R^2 - \frac{y^2}{\tilde{C}} \left(1 - \frac{\tilde{B}^2}{4\tilde{C}} \right)}}{R \left(c_A \sqrt{1 - \frac{\tilde{B}^2}{4\tilde{C}}} \right)} \leq \frac{1}{\left(c_A \sqrt{1 - \frac{\tilde{B}^2}{4\tilde{C}}} \right)} = \frac{1}{v_{\text{crit}}},\tag{2.17}$$

which incidentally is one over the critical velocity in the steady-state limit [20]; we will come back to this point when we study limits of the more general solution we are presently deriving.

The integral over the entire imaginary axis of p becomes a difference of integrals over the positive imaginary axes of p_{\pm} , and we close the path by adding the integrals over $\tau \in [\tau_{\min}, \infty)$ and by connecting them at $p = \pm i\infty$ where the integrand is zero due to

$$\lim_{p \rightarrow \pm i\infty} e^{-s\beta|y|} \approx \lim_{p \rightarrow \pm i\infty} \exp \left(-s|y| \sqrt{-p^2} \sqrt{\frac{1}{\tilde{C}} \left(1 - \frac{\tilde{B}^2}{4\tilde{C}} \right)} - sy \frac{\tilde{B}p}{2\tilde{C}} \right) \rightarrow 0,\tag{2.18}$$

since $(-p^2) \rightarrow +\infty$ and the second term in the argument of the exponential is purely imaginary and hence bounded by 1. By Cauchy's theorem, the integral over the closed path is given by the sum of residua within that path. In the present case we have poles at $p = 0$ in the first term of $\partial_y \mathcal{L}\{u\}(x, y, s)$ and at $p = \eta'(x)$ in the second term of both $\partial_x \mathcal{L}\{u\}(x, y, s)$ and $\partial_y \mathcal{L}\{u\}(x, y, s)$. The latter need only be taken into account if $\eta'(x) \leq |p_0|$ as noted above in (2.17), and we can ensure this by multiplying the corresponding residuum by an according step function. The three residuum terms we need are straightforwardly computed to be:

$$\mathcal{R}_0 = 2\pi i \lim_{\epsilon' \rightarrow 0^+} \text{Res} \left(\frac{-ib}{4\pi} \left(\frac{\beta}{(p - \epsilon')} \right) e^{-s\beta|y|} e^{-spx} \right) = \frac{b}{2c_A \sqrt{\tilde{C}}} e^{-s|y|/(c_A \sqrt{\tilde{C}})},\tag{2.19a}$$

$$\begin{aligned}
\mathcal{R}_x &= 2\pi i \text{Res} \left[\frac{-ib \text{sgn}(y)}{4\pi} e^{-spx} e^{-s\beta|y|} \frac{p}{\eta'(x) - p} \right] \\
&= \frac{b \text{sgn}(y)}{2} \eta'(x) e^{-sx\eta'(x)} \exp \left[-s \left(|y| \sqrt{\frac{1}{c_A^2 \tilde{C}} - \frac{(\eta'(x))^2}{\tilde{C}}} \left(1 - \frac{\tilde{B}^2}{4\tilde{C}} \right) - y \frac{\tilde{B}\eta'(x)}{2\tilde{C}}} \right) \right], \quad (2.19b)
\end{aligned}$$

$$\begin{aligned}
\mathcal{R}_y &= 2\pi i \text{Res} \left[\frac{-ib}{4\pi} e^{-spx} e^{-s\beta|y|} \frac{\beta}{\eta'(x) - p} \right] \\
&= \frac{b}{2} \left(\sqrt{\frac{1}{c_A^2 \tilde{C}} - \frac{(\eta'(x))^2}{\tilde{C}}} \left(1 - \frac{\tilde{B}^2}{4\tilde{C}} \right) - \text{sgn}(y) \frac{\tilde{B}\eta'(x)}{2\tilde{C}}} \right) e^{-sx\eta'(x)} \\
&\quad \times \exp \left[-s \left(|y| \sqrt{\frac{1}{c_A^2 \tilde{C}} - \frac{(\eta'(x))^2}{\tilde{C}}} \left(1 - \frac{\tilde{B}^2}{4\tilde{C}} \right) - y \frac{\tilde{B}\eta'(x)}{2\tilde{C}}} \right) \right]. \quad (2.19c)
\end{aligned}$$

We see that the square root inside the exponentials of \mathcal{R}_x and \mathcal{R}_y becomes imaginary for $\eta'(x) > 1/(c_A \sqrt{1 - \frac{\tilde{B}^2}{4\tilde{C}}})$. For $x - y \frac{\tilde{B}}{2\tilde{C}} > 0$, the closed path is counter clockwise, meaning these residua must be subtracted from the integral over τ in order to equal the integral over the imaginary axis of p . Otherwise, the path is clockwise and the residua need to be added, in other words we add the residua multiplied by $\text{sgn}(y \frac{\tilde{B}}{2\tilde{C}} - x)$.

In rewriting the integrand as a function of τ we will also need $\beta(\tau)$ and $dp(\tau)$. From $\tau = (\beta|y| + px)$ we deduce

$$\beta_{\pm} = \frac{1}{|y|} (\tau - p_{\pm}x) = \frac{1}{R^2} \left[\tau \left(\frac{|y|}{\tilde{C}} - x \frac{\text{sgn}(y)\tilde{B}}{2\tilde{C}} \right) \mp ix \sqrt{\tau^2 \frac{1}{\tilde{C}} \left(1 - \frac{\tilde{B}^2}{4\tilde{C}} \right) - \frac{R^2}{c_A^2 \tilde{C}}} \right], \quad (2.20)$$

and

$$dp_{\pm} = \frac{1}{R^2} \left(x - y \frac{\tilde{B}}{2\tilde{C}} \pm i|y| \frac{\frac{\tau}{\tilde{C}} \left(1 - \frac{\tilde{B}^2}{4\tilde{C}} \right)}{\sqrt{\tau^2 \frac{1}{\tilde{C}} \left(1 - \frac{\tilde{B}^2}{4\tilde{C}} \right) - \frac{R^2}{c_A^2 \tilde{C}}}} \right) d\tau. \quad (2.21)$$

All integrals over p now take the general form

$$\int_{\tau_{\min}}^{\infty} dp_{+}(\tau) f(\tau) - \int_{\tau_{\min}}^{\infty} dp_{-}(\tau) f^{*}(\tau) = \frac{i}{2} \Im \left(\int_{\tau_{\min}}^{\infty} dp_{+}(\tau) f(\tau) \right) + \text{sgn} \left(y \frac{\tilde{B}}{2\tilde{C}} - x \right) \mathcal{R}. \quad (2.22)$$

In particular,

$$\begin{aligned}
\partial_x \mathcal{L}\{u\}(x, y, s) &= \frac{b \text{sgn}(y)}{2\pi} \left[\Im \left(\int_{\tau_{\min}}^{\infty} dp_{+}(\tau) e^{-s\tau} \right) + e^{-s(\eta(x) - x\eta'(x))} \Im \left(\int_{\tau_{\min}}^{\infty} dp_{+}(\tau) e^{-s\tau} \frac{p_{+}\eta'(x) - |p|^2}{|\eta'(x) - p|^2} \right) \right. \\
&\quad \left. + \int_0^{\infty} dx' (e^{-s\eta(x')} - e^{-s\tilde{\eta}}) s \Im \left(\int_{\tau'_{\min}}^{\infty} dp'_{+}(\tau') e^{-s\tau'} p'_{+} \right) \right] \\
&\quad + \text{sgn} \left(y \frac{\tilde{B}}{2\tilde{C}} - x \right) \Theta(p_0 - \eta'(x)) \mathcal{R}_x, \quad (2.23a)
\end{aligned}$$

$$\begin{aligned}
\partial_y \mathcal{L}\{u\}(x, y, s) = & \frac{-b}{2\pi} \left[\Im \left(\int_{\tau_{\min}}^{\infty} dp_+(\tau) e^{-s\tau} \frac{\beta_+ p_-}{|p|^2} \right) + e^{-s(\eta(x) - x\eta'(x))} \Im \left(\int_{\tau_{\min}}^{\infty} dp_+(\tau) e^{-s\tau} \frac{\beta_+(\eta'(x) - p_-)}{|\eta'(x) - p|^2} \right) \right. \\
& \left. + \int_0^{\infty} dx' \left(e^{-s\eta(x')} - e^{-s\tilde{\eta}} \right) s \Im \left(\int_{\tau'_{\min}}^{\infty} dp'_+(\tau') e^{-s\tau'} \beta'_+ \right) \right] \\
& + \operatorname{sgn} \left(y \frac{\tilde{B}}{2\tilde{C}} - x \right) (\mathcal{R}_0 + \Theta(p_0 - \eta'(x)) \mathcal{R}_y), \tag{2.23b}
\end{aligned}$$

where the primed quantities p'_\pm , β'_\pm , and τ'_{\min} differ from their unprimed counterparts only by $x \rightarrow (x - x')$. Using the expressions listed in Appendix B for $\Im(dp_+ p_-)$, $\Im(dp_+ \beta_+ p_-)$, $\Im(dp_+ \beta_+)$, $|\eta'(x) - p|^2$, and $|p|^2$ in terms of τ , we find

$$\begin{aligned}
\partial_x \mathcal{L}\{u\}(x, y, s) = & \frac{by}{2\pi} \int_0^{\infty} d\tau e^{-s\tau} \frac{\Theta(\tau - \tau_{\min})}{R^2 \sqrt{\frac{1}{\tilde{C}} \left(1 - \frac{\tilde{B}^2}{4\tilde{C}}\right) - \frac{R^2}{\tau^2 c_A^2 \tilde{C}}}} \left\{ \frac{1}{\tilde{C}} \left(1 - \frac{\tilde{B}^2}{4\tilde{C}}\right) \right. \\
& \left. + e^{-s(\eta(x) - x\eta'(x))} \frac{\left[\tau \eta'(x) \left(x - y \frac{\tilde{B}}{2\tilde{C}}\right) \frac{1}{\tilde{C}} \left[2 \left(1 - \frac{\tilde{B}^2}{4\tilde{C}}\right) - \frac{R^2}{\tau^2 c_A^2 \tilde{C}} \right] - \left(\tau^2 - \frac{y^2}{c_A^2 \tilde{C}}\right) \frac{1}{\tilde{C}} \left(1 - \frac{\tilde{B}^2}{4\tilde{C}}\right) \right]}{\left(\tau^2 - \frac{y^2}{c_A^2 \tilde{C}} - 2\tau \eta'(x) \left(x - y \frac{\tilde{B}}{2\tilde{C}}\right) + (\eta'(x))^2 R^2\right)} \right\} \\
& + \frac{b}{2\pi} \int_0^{\infty} dx' s \int_0^{\infty} d\tau e^{-s\tau} \Theta(\tau - \tau'_{\min}) \left(e^{-s\eta(x')} - e^{-s\tilde{\eta}} \right) \frac{\tau y \left(x - x' - y \frac{\tilde{B}}{2\tilde{C}}\right) \left(2 \left(1 - \frac{\tilde{B}^2}{4\tilde{C}}\right) - \frac{R'^2}{\tau^2 c_A^2 \tilde{C}}\right)}{\tilde{C} R'^4 \sqrt{\frac{1}{\tilde{C}} \left(1 - \frac{\tilde{B}^2}{4\tilde{C}}\right) - \frac{R'^2}{\tau^2 c_A^2 \tilde{C}}}} \\
& + \operatorname{sgn} \left(y \frac{\tilde{B}}{2\tilde{C}} - x \right) \Theta(p_0 - \eta'(x)) \mathcal{R}_x, \tag{2.24a}
\end{aligned}$$

$$\begin{aligned}
\partial_y \mathcal{L}\{u\}(x, y, s) = & \frac{b}{2\pi} \int_0^{\infty} d\tau e^{-s\tau} \frac{\Theta(\tau - \tau_{\min})}{R^2 \sqrt{\frac{1}{\tilde{C}} \left(1 - \frac{\tilde{B}^2}{4\tilde{C}}\right) - \frac{R^2}{\tau^2 c_A^2 \tilde{C}}}} \left\{ \frac{1}{\tilde{C}} \left[\frac{R^2}{c_A^2} \frac{\left(x - y \frac{\tilde{B}}{2\tilde{C}}\right)}{\left(\tau^2 - \frac{y^2}{c_A^2 \tilde{C}}\right)} - x \left(1 - \frac{\tilde{B}^2}{4\tilde{C}}\right) \right] \right. \\
& + \frac{e^{-s(\eta(x) - x\eta'(x))}}{\left(\tau^2 - \frac{y^2}{c_A^2 \tilde{C}} - 2\tau \eta'(x) \left(x - y \frac{\tilde{B}}{2\tilde{C}}\right) + (\eta'(x))^2 R^2\right)} \left[\frac{\tau \eta'(x)}{\tilde{C}} \left[\left(\frac{y^2}{\tilde{C}} - x^2\right) \left(1 - \frac{\tilde{B}^2}{4\tilde{C}}\right) + x \left(x - y \frac{\tilde{B}}{2\tilde{C}}\right) \frac{R^2}{\tau^2 c_A^2 \tilde{C}} \right] \right. \\
& \left. \left. - \frac{1}{\tilde{C}} \left[\frac{R^2}{c_A^2} \left(x - y \frac{\tilde{B}}{2\tilde{C}}\right) - x \left(\tau^2 - \frac{y^2}{c_A^2 \tilde{C}}\right) \left(1 - \frac{\tilde{B}^2}{4\tilde{C}}\right) \right] \right] \right\} \\
& + \frac{b}{2\pi} \int_0^{\infty} dx' s \int_0^{\infty} d\tau e^{-s\tau} \Theta(\tau - \tau'_{\min}) \left(e^{-s\eta(x')} - e^{-s\tilde{\eta}} \right) \frac{\tau}{R'^4 \tilde{C} \sqrt{\frac{1}{\tilde{C}} \left(1 - \frac{\tilde{B}^2}{4\tilde{C}}\right) - \frac{R'^2}{\tau^2 c_A^2 \tilde{C}}}} \\
& \times \left[\left(\frac{y^2}{\tilde{C}} - (x - x')^2\right) \left(1 - \frac{\tilde{B}^2}{4\tilde{C}}\right) + (x - x') \left(x - x' - y \frac{\tilde{B}}{2\tilde{C}}\right) \frac{R'^2}{\tau^2 c_A^2 \tilde{C}} \right] \\
& + \operatorname{sgn} \left(y \frac{\tilde{B}}{2\tilde{C}} - x \right) (\mathcal{R}_0 + \Theta(p_0 - \eta'(x)) \mathcal{R}_y), \tag{2.24b}
\end{aligned}$$

with $\tau_{\min} = R / \left(c_A \sqrt{1 - \frac{\tilde{B}^2}{4\tilde{C}}}\right)$. The inverse Laplace transform can almost be read off from the expressions above, considering the following properties of Laplace transforms [42]:

- multiplication by e^{-sT} corresponds to a translation in time by T and
- multiplication by s corresponds to a time derivative (plus boundary terms which in this case cancel the $\partial_t \Theta(\dots)$ term).

Putting all the pieces together our general solution in the anisotropic case is

$$\begin{aligned}
\partial_x u_z(x, y, t) = & \frac{b}{2\pi} \partial_t \int_0^\infty dx' \left(\mathcal{F}_x [\eta(x'), \tilde{t}, t] - \mathcal{F}_x [\eta(x) + (x' - x)\eta'(x), \tilde{t}, t] \right) \Big|_{\tilde{t}=t} \\
& + \frac{b}{2\pi} \frac{y}{R^2} \left[\Theta \left(t - \frac{R}{c_A \sqrt{1 - \frac{\tilde{B}^2}{4\tilde{C}}}} \right) \frac{\frac{1}{\tilde{C}} \left(1 - \frac{\tilde{B}^2}{4\tilde{C}} \right)}{\sqrt{\frac{1}{\tilde{C}} \left(1 - \frac{\tilde{B}^2}{4\tilde{C}} \right) - \frac{R^2}{t^2 c_A^2 \tilde{C}}}} \right. \\
& \quad \left. + \Theta \left(\tau - \frac{R}{c_A \sqrt{1 - \frac{\tilde{B}^2}{4\tilde{C}}}} \right) \frac{\left[\tau \eta'(x) \left(x - y \frac{\tilde{B}}{2\tilde{C}} \right) \frac{1}{\tilde{C}} \left[2 \left(1 - \frac{\tilde{B}^2}{4\tilde{C}} \right) - \frac{R^2}{\tau^2 c_A^2 \tilde{C}} \right] - \left(\tau^2 - \frac{y^2}{c_A^2 \tilde{C}} \right) \frac{1}{\tilde{C}} \left(1 - \frac{\tilde{B}^2}{4\tilde{C}} \right) \right]}{\sqrt{\frac{1}{\tilde{C}} \left(1 - \frac{\tilde{B}^2}{4\tilde{C}} \right) - \frac{R^2}{\tau^2 c_A^2 \tilde{C}} \left(\tau^2 - \frac{y^2}{c_A^2 \tilde{C}} - 2\tau \eta'(x) \left(x - y \frac{\tilde{B}}{2\tilde{C}} \right) + (\eta'(x))^2 R^2 \right)}} \right] \\
& + \frac{b \operatorname{sgn}(y)}{2} \operatorname{sgn} \left(y \frac{\tilde{B}}{2\tilde{C}} - x \right) \eta'(x) \Theta(p_0 - \eta'(x)) \delta \left(t - x \eta'(x) - \left(|y| \sqrt{\frac{1}{c_A^2 \tilde{C}} - \frac{(\eta'(x))^2}{\tilde{C}} \left(1 - \frac{\tilde{B}^2}{4\tilde{C}} \right)} - y \frac{\tilde{B} \eta'(x)}{2\tilde{C}} \right) \right),
\end{aligned} \tag{2.25a}$$

$$\begin{aligned}
\partial_y u_z(x, y, t) = & \frac{b}{2\pi} \partial_t \int_0^\infty dx' \left(\mathcal{F}_y [\eta(x'), \tilde{t}, t] - \mathcal{F}_y [\eta(x) + (x' - x)\eta'(x), \tilde{t}, t] \right) \Big|_{\tilde{t}=t} + \frac{b \operatorname{sgn} \left(y \frac{\tilde{B}}{2\tilde{C}} - x \right)}{2c_A \sqrt{\tilde{C}}} \delta \left(t - \frac{|y|}{c_A \sqrt{\tilde{C}}} \right) \\
& + \frac{b}{2\pi} \frac{1}{R^2} \left\{ \Theta \left(t - \frac{R}{c_A \sqrt{1 - \frac{\tilde{B}^2}{4\tilde{C}}}} \right) \frac{\frac{1}{\tilde{C}} \left[\frac{R^2}{c_A^2 \tilde{C}} \left(x - y \frac{\tilde{B}}{2\tilde{C}} \right) - x \left(t^2 - \frac{y^2}{c_A^2 \tilde{C}} \right) \left(1 - \frac{\tilde{B}^2}{4\tilde{C}} \right) \right]}{\sqrt{\frac{1}{\tilde{C}} \left(1 - \frac{\tilde{B}^2}{4\tilde{C}} \right) - \frac{R^2}{t^2 c_A^2 \tilde{C}} \left(t^2 - \frac{y^2}{c_A^2 \tilde{C}} \right)}} \right. \\
& \quad \left. + \Theta \left(\tau - \frac{R}{c_A \sqrt{1 - \frac{\tilde{B}^2}{4\tilde{C}}}} \right) \frac{\tau \eta'(x) \left(\frac{y^2}{\tilde{C}} - x^2 \right) \left(1 - \frac{\tilde{B}^2}{4\tilde{C}} \right) + \left(\frac{x \eta'(x)}{\tau} - 1 \right) \frac{R^2}{c_A^2 \tilde{C}} \left(x - y \frac{\tilde{B}}{2\tilde{C}} \right) + x \left(\tau^2 - \frac{y^2}{c_A^2 \tilde{C}} \right) \left(1 - \frac{\tilde{B}^2}{4\tilde{C}} \right)}{\tilde{C} \sqrt{\frac{1}{\tilde{C}} \left(1 - \frac{\tilde{B}^2}{4\tilde{C}} \right) - \frac{R^2}{\tau^2 c_A^2 \tilde{C}} \left(\tau^2 - \frac{y^2}{c_A^2 \tilde{C}} - 2\tau \eta'(x) \left(x - y \frac{\tilde{B}}{2\tilde{C}} \right) + (\eta'(x))^2 R^2 \right)}} \right\} \\
& + \frac{b}{2} \operatorname{sgn} \left(y \frac{\tilde{B}}{2\tilde{C}} - x \right) \left(\sqrt{\frac{1}{c_A^2 \tilde{C}} - \frac{(\eta'(x))^2}{\tilde{C}} \left(1 - \frac{\tilde{B}^2}{4\tilde{C}} \right)} - \operatorname{sgn}(y) \frac{\tilde{B} \eta'(x)}{2\tilde{C}} \right) \Theta(p_0 - \eta'(x)) \\
& \quad \times \delta \left(t - x \eta'(x) - \left(|y| \sqrt{\frac{1}{c_A^2 \tilde{C}} - \frac{(\eta'(x))^2}{\tilde{C}} \left(1 - \frac{\tilde{B}^2}{4\tilde{C}} \right)} - y \frac{\tilde{B} \eta'(x)}{2\tilde{C}} \right) \right),
\end{aligned} \tag{2.25b}$$

with

$$\mathcal{F}_x [\eta, \tilde{t}, t] = \Theta \left(\tilde{t} - \eta - \frac{R'}{c_A \sqrt{1 - \frac{\tilde{B}^2}{4\tilde{C}}}} \right) \frac{y \left(x - x' - y \frac{\tilde{B}}{2\tilde{C}} \right) \left(\frac{2}{\tilde{C}} \left(1 - \frac{\tilde{B}^2}{4\tilde{C}} \right) (t - \eta)^2 - \frac{R'^2}{c_A^2 \tilde{C}} \right)}{R'^4 \sqrt{\frac{1}{\tilde{C}} \left(1 - \frac{\tilde{B}^2}{4\tilde{C}} \right) (t - \eta)^2 - \frac{R'^2}{c_A^2 \tilde{C}}}}, \tag{2.26a}$$

$$\mathcal{F}_y[\eta, \tilde{t}, t] = \Theta\left(\tilde{t} - \eta - \frac{R'}{c_A \sqrt{1 - \frac{\tilde{B}^2}{4\tilde{C}}}}\right) \frac{\left(\frac{y^2}{\tilde{C}} - (x - x')^2\right) \frac{1}{\tilde{C}} \left(1 - \frac{\tilde{B}^2}{4\tilde{C}}\right) (t - \eta)^2 + (x - x') \left(x - x' - y \frac{\tilde{B}}{2\tilde{C}}\right) \frac{R'^2}{c_A^2 \tilde{C}}}{R'^4 \sqrt{\frac{1}{\tilde{C}} \left(1 - \frac{\tilde{B}^2}{4\tilde{C}}\right) (t - \eta)^2 - \frac{R'^2}{c_A^2 \tilde{C}}}}, \quad (2.26b)$$

and

$$\begin{aligned} R^2 &= \left(x^2 - xy \frac{\tilde{B}}{\tilde{C}} + \frac{y^2}{\tilde{C}}\right), & R'^2 &= \left((x - x')^2 - (x - x')y \frac{\tilde{B}}{\tilde{C}} + \frac{y^2}{\tilde{C}}\right), & \tau &= t - (\eta(x) - x\eta'(x)), \\ p_0 &= \frac{x - y \frac{\tilde{B}}{2\tilde{C}}}{R c_A \sqrt{1 - \frac{\tilde{B}^2}{4\tilde{C}}}}. \end{aligned} \quad (2.27)$$

As noted earlier, $\mathcal{F}_x(\eta)$ and $\mathcal{F}_y(\eta)$ exhibit quadratic divergences at $y \rightarrow 0$ and $x' \rightarrow x$ (for $y \neq 0$, R' never vanishes for real x' since $\tilde{B}^2/(4\tilde{C}) < 1$). These poles are subtracted by $\mathcal{F}_x(\tilde{\eta})$ and $\mathcal{F}_y(\tilde{\eta})$: Since $\tilde{\eta}$ is the linear order Taylor expansion of η around $x' = x$, the linear order Taylor expansions of $\mathcal{F}_x(\eta)$ and $\mathcal{F}_x(\tilde{\eta})$ (and likewise $\mathcal{F}_y(\eta)$ and $\mathcal{F}_y(\tilde{\eta})$) are equal to one another, thereby cancelling the leading quadratic and subleading linear poles. This leaves at most only an integrable logarithmic pole and hence the terms integrated over x' are rendered finite. Notice that the derivative with respect to time must be performed after the integration over x' : exchanging the order would result in a divergent x' integral due to the square root in the denominator of \mathcal{F} which is zero when the argument of the step function is zero, i.e. prior to taking the time derivative we have an integrable pole at one edge of the integration domain — see also Refs. [37, 43] for a discussion on this point.

2.2 Constant velocity

The simplest case one can study within the general solution (2.25) is a dislocation at rest at time $t < 0$ which suddenly starts moving at constant velocity v from $t \geq 0$. Then

$$\begin{aligned} \eta(x) &= \text{sgn}(x) \eta(|x|) = \frac{x}{v}, & \eta'(x) &= \frac{1}{v}, & \tau &= t - (\eta(x) - x\eta'(x)) = t, \\ \tilde{\eta} &= \frac{x'}{v} = \eta(x'), \end{aligned} \quad (2.28)$$

i.e. all the $\mathcal{F}(\eta)$ terms cancel one another identically and the shift in time variable τ is zero allowing for further simplifications of the remaining terms:

$$\begin{aligned} \partial_x u_z^v(x, y, t) &= \frac{b}{2\pi} \Theta\left(t - \frac{R}{c_A \sqrt{1 - \frac{\tilde{B}^2}{4\tilde{C}}}}\right) \frac{y \frac{1}{\tilde{C}} \left[\left(1 - \frac{\tilde{B}^2}{4\tilde{C}}\right) - \left(x - y \frac{\tilde{B}}{2\tilde{C}}\right) \frac{v}{t c_A^2}\right]}{\sqrt{\frac{1}{\tilde{C}} \left(1 - \frac{\tilde{B}^2}{4\tilde{C}}\right) - \frac{R^2}{t^2 c_A^2 \tilde{C}} \left(v^2 t^2 - \frac{y^2 v^2}{c_A^2 \tilde{C}} - 2vt \left(x - y \frac{\tilde{B}}{2\tilde{C}}\right) + R^2\right)}} \\ &\quad + \frac{b \text{sgn}(y)}{2} \text{sgn}\left(y \frac{\tilde{B}}{2\tilde{C}} - x\right) \Theta\left(p_0 - \frac{1}{v}\right) \delta\left(x - vt + |y| \sqrt{\frac{v^2}{c_A^2 \tilde{C}} - \frac{1}{\tilde{C}} \left(1 - \frac{\tilde{B}^2}{4\tilde{C}}\right)} - y \frac{\tilde{B}}{2\tilde{C}}\right), \end{aligned} \quad (2.29a)$$

$$\begin{aligned}
\partial_y u_z^v(x, y, t) = & \frac{b \operatorname{sgn}(-x)}{2c_A \sqrt{\tilde{C}}} \delta \left(t - \frac{|y|}{c_A \sqrt{\tilde{C}}} \right) \\
& + \frac{b}{2\pi} \Theta \left(t - \frac{R}{c_A \sqrt{1 - \frac{\tilde{B}^2}{4\tilde{C}}}} \right) \frac{1}{R^2 \sqrt{\frac{1}{\tilde{C}} \left(1 - \frac{\tilde{B}^2}{4\tilde{C}} \right) - \frac{R^2}{t^2 c_A^2 \tilde{C}}}} \left\{ \frac{\frac{vt}{\tilde{C}} \left[\left(\frac{y^2}{\tilde{C}} - x^2 \right) \left(1 - \frac{\tilde{B}^2}{4\tilde{C}} \right) + x \left(x - y \frac{\tilde{B}}{2\tilde{C}} \right) \frac{R^2}{t^2 c_A^2} \right]}{\left(v^2 t^2 - \frac{y^2 v^2}{c_A^2 \tilde{C}} - 2tv \left(x - y \frac{\tilde{B}}{2\tilde{C}} \right) + R^2 \right)} \right. \\
& \left. + \frac{\frac{1}{\tilde{C}} \left[\frac{R^2}{c_A^2} \left(x - y \frac{\tilde{B}}{2\tilde{C}} \right) - x \left(t^2 - \frac{y^2}{c_A^2 \tilde{C}} \right) \left(1 - \frac{\tilde{B}^2}{4\tilde{C}} \right) \right] \left(R^2 - 2vt \left(x - y \frac{\tilde{B}}{2\tilde{C}} \right) \right)}{\left(t^2 - \frac{y^2}{c_A^2 \tilde{C}} \right) \left(v^2 t^2 - \frac{y^2 v^2}{c_A^2 \tilde{C}} - 2vt \left(x - y \frac{\tilde{B}}{2\tilde{C}} \right) + R^2 \right)} \right\} \\
& + \frac{b}{2} \operatorname{sgn} \left(y \frac{\tilde{B}}{2\tilde{C}} - x \right) \left(\sqrt{\frac{v^2}{c_A^2 \tilde{C}} - \frac{1}{\tilde{C}} \left(1 - \frac{\tilde{B}^2}{4\tilde{C}} \right)} - \operatorname{sgn}(y) \frac{\tilde{B}}{2\tilde{C}} \right) \Theta \left(p_0 - \frac{1}{v} \right) \\
& \times \delta \left(x - vt + |y| \sqrt{\frac{v^2}{c_A^2 \tilde{C}} - \frac{1}{\tilde{C}} \left(1 - \frac{\tilde{B}^2}{4\tilde{C}} \right)} - y \frac{\tilde{B}}{2\tilde{C}} \right). \tag{2.29b}
\end{aligned}$$

The sudden jump from static to constant motion is of course unphysical, but in the large time limit the present expression must tend to the steady state solution. This limit must be taken carefully, taking into account that the dislocation has moved in the x direction by $v\delta t$ in every time interval δt . Hence, we introduce coordinate $x' := x - vt$ which moves with the dislocation, and take $t \rightarrow \infty$ while keeping x' fixed, i.e. all occurrences of x must be replaced by $x = x' + vt$ prior to taking t to infinity. Using

$$\begin{aligned}
\lim_{t \rightarrow \infty} \Theta \left(t - \frac{R}{c_A \sqrt{1 - \frac{\tilde{B}^2}{4\tilde{C}}}} \right) &= \lim_{t \rightarrow \infty} \Theta \left(t - \frac{vt}{c_A \sqrt{1 - \frac{\tilde{B}^2}{4\tilde{C}}}} \right) = \Theta \left(1 - \frac{v}{c_A \sqrt{1 - \frac{\tilde{B}^2}{4\tilde{C}}}} \right), \\
\lim_{t \rightarrow \infty} \Theta \left(p_0 - \frac{1}{v} \right) &= \Theta \left(\frac{1}{c_A \sqrt{1 - \frac{\tilde{B}^2}{4\tilde{C}}}} - \frac{1}{v} \right), \tag{2.30}
\end{aligned}$$

we find after some algebra:

$$\begin{aligned}
\lim_{t \rightarrow \infty} \partial_{x'} u_z^v(x(x', t), y, t) &= \frac{b}{2\pi} \Theta \left(1 - \frac{v}{c_A \sqrt{1 - \frac{\tilde{B}^2}{4\tilde{C}}}} \right) \frac{y \sqrt{\frac{1}{\tilde{C}} \left(1 - \frac{\tilde{B}^2}{4\tilde{C}} - \frac{v^2}{c_A^2} \right)}}{\left(x' - \frac{\tilde{B}}{2\tilde{C}} y \right)^2 + y^2 \frac{1}{\tilde{C}} \left(1 - \frac{\tilde{B}^2}{4\tilde{C}} - \frac{v^2}{c_A^2} \right)} \\
&\quad - \frac{b \operatorname{sgn}(y)}{2} \delta \left(x' + |y| \sqrt{\frac{v^2}{c_A^2 \tilde{C}} - \frac{1}{\tilde{C}} \left(1 - \frac{\tilde{B}^2}{4\tilde{C}} \right)} - y \frac{\tilde{B}}{2\tilde{C}} \right), \tag{2.31a}
\end{aligned}$$

$$\begin{aligned}
\lim_{t \rightarrow \infty} \partial_y u_z^v(x(x', t), y, t) &= \frac{b}{2\pi} \Theta \left(1 - \frac{v}{c_A \sqrt{1 - \frac{\tilde{B}^2}{4\tilde{C}}}} \right) \frac{-x' \sqrt{\frac{1}{\tilde{C}} \left(1 - \frac{\tilde{B}^2}{4\tilde{C}} - \frac{v^2}{c_A^2} \right)}}{\left(x' - \frac{\tilde{B}}{2\tilde{C}} y \right)^2 + y^2 \frac{1}{\tilde{C}} \left(1 - \frac{\tilde{B}^2}{4\tilde{C}} - \frac{v^2}{c_A^2} \right)} \\
&\quad - \frac{b}{2} \left(\sqrt{\frac{v^2}{c_A^2 \tilde{C}} - \frac{1}{\tilde{C}} \left(1 - \frac{\tilde{B}^2}{4\tilde{C}} \right)} - \operatorname{sgn}(y) \frac{\tilde{B}}{2\tilde{C}} \right) \delta \left(x' + |y| \sqrt{\frac{v^2}{c_A^2 \tilde{C}} - \frac{1}{\tilde{C}} \left(1 - \frac{\tilde{B}^2}{4\tilde{C}} \right)} - y \frac{\tilde{B}}{2\tilde{C}} \right). \tag{2.31b}
\end{aligned}$$

Notice, the presence of a ‘critical’ velocity

$$v_{\text{crit}} = c_A \sqrt{1 - \frac{\tilde{B}^2}{4\tilde{C}}}, \quad (2.32)$$

which separates a ‘subsonic’ from a ‘supersonic’ regime. As emphasized in Ref. [20], v_{crit} is in general *different* from any sound speed moving in the direction parallel to the dislocation. In particular, the solution (2.31) diverges at the contours $x' = \frac{\tilde{B}}{2\tilde{C}}y$ when the velocity reaches v_{crit} .

At all subsonic speeds, $v < v_{\text{crit}}$ the delta functions vanish identically for all real x' and y since the square roots in their arguments become imaginary. Therefore, the step function ensuring supersonic motion in those terms could be dropped above. Integrating any of the latter two expressions with respect to x' or y in the strictly subsonic regime yields the solution for (subsonic) u_z in the stationary limit³:

$$\lim_{t \rightarrow \infty} u_z^v(x(x', t), y, t) = \frac{b}{2\pi} \arctan \left(\frac{y \sqrt{\frac{1}{\tilde{C}} \left(1 - \frac{\tilde{B}^2}{4\tilde{C}} - \frac{v^2}{c_A^2} \right)}}{-x' + \frac{\tilde{B}}{2\tilde{C}}y} \right), \quad (2.33)$$

which coincides (as expected) with the solution discussed in [20]. Upon plugging in the expressions (A.4) for fcc slip systems the static limit ($v \rightarrow 0$) of the solution above coincides with what was derived in Ref. [33, Eq. (13-128)].

2.3 Special case of constant acceleration

Let us now assume again the dislocation is at rest at time $t < 0$ and starts to accelerate at a constant rate a from $t \geq 0$. Then $l(t) = \frac{a}{2}t^2 > 0$ and hence

$$\begin{aligned} \eta(x) &= \text{sgn}(x) \sqrt{\frac{2|x|}{a}}, & \eta'(x) &= \text{sgn}(x) \partial_x \eta(|x|) = \frac{\eta(x)}{2x}, & \tau &= t - (\eta(x) - x\eta'(x)) = t - \frac{1}{2}\eta(x), \\ \tilde{\eta} &= \frac{1}{2} \left(1 + \frac{x'}{x} \right) \eta(x). \end{aligned} \quad (2.34)$$

Because the current velocity is given by $v(t) = at$, the transition from subsonic to supersonic in the above solution happens when $t = v_{\text{crit}}/a$. At this point, the dislocation has traveled a distance $x = v_{\text{crit}}^2/(2a)$, and it is at this position where it is most obvious that the core-singularity at $y = 0$ is enhanced within $\partial_y u_z$. Furthermore, like in the constant velocity case there are contours where the solution diverges when the critical velocity is reached. Those contours follow from⁴

$$\begin{aligned} 0 &= \tau^2 - \frac{y^2}{c_A^2 \tilde{C}} - 2\tau\eta' \left(x - y \frac{\tilde{B}}{2\tilde{C}} \right) + \eta'^2 R^2 \\ &= \left[\tau - \eta' \left(x - y \frac{\tilde{B}}{2\tilde{C}} \right) \right]^2 + \left(\eta'^2 - \frac{1}{v_{\text{crit}}^2} \right) \frac{y^2}{\tilde{C}} \left(1 - \frac{\tilde{B}}{4\tilde{C}} \right), \end{aligned} \quad (2.35)$$

³ A note regarding the definition of the $\arctan()$ function is in order: We adopt here the most common definition (i.e. the IEEE convention) where $\arctan(y/x) \in [0, +\pi]$ in the first and second quadrant and $\arctan(y/x) \in [-\pi, 0]$ in the third and fourth quadrant. Ref. [33] in contrast uses the less common definition $\arctan(y/x) = \phi$, $\forall \phi \in [0, 2\pi]$, and this is the reason we have an overall minus sign in front of the denominator of the argument of the arc-tangent in Eq. (2.33) rather than an overall sign in front of the $\arctan()$ like in Ref. [33, Eq. (13-128)].

⁴We see immediately, that in the constant velocity limit the second term is zero as $\eta' = 1/v \rightarrow 1/v_{\text{crit}}$, and the first term vanishes for the contour $(x - vt) = y \frac{\tilde{B}}{2\tilde{C}}$ since $\tau = t$ in that case.

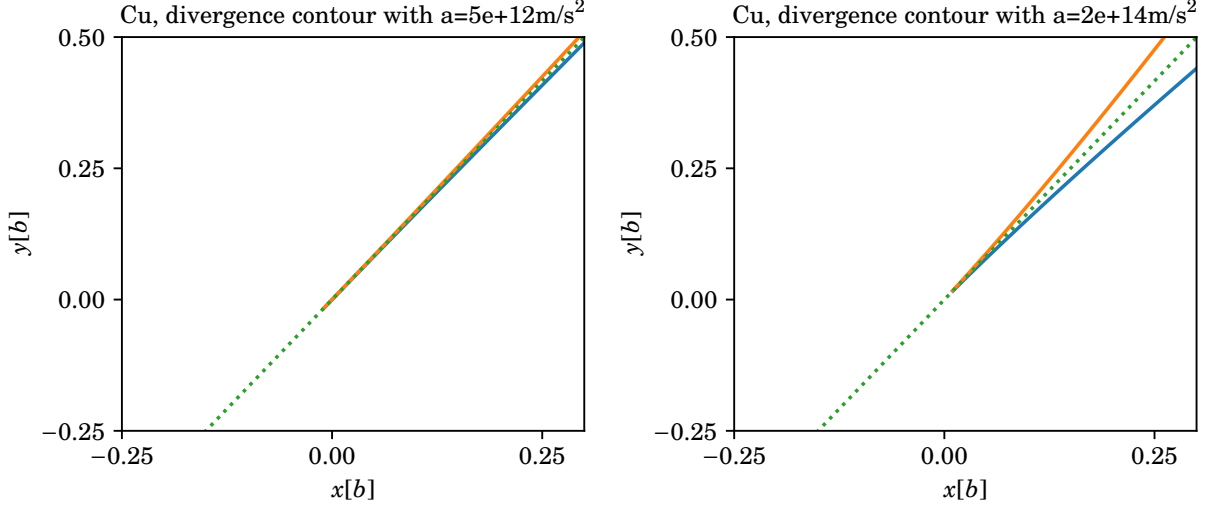


Figure 2: We show the contours $y(x)$ where $\partial_x u_z$, $\partial_y u_z$ diverge when reaching the critical velocity $v(t) = v_{\text{crit}}$ (solid lines) at the example of copper ($\rho = 8.96 \text{ g/ccm}$, $b = 2.56 \text{ \AA}$, $c_{44} = 75.7 \text{ GPa}$, and $c' = 23.55 \text{ GPa}$, see [20, 44]) for two different values for acceleration a . For comparison, the dotted line shows what the contour looks like in the constant velocity case. We see that for small acceleration a , the two solid lines almost collapse to the dotted line in the positive x , y region, but for non-vanishing acceleration they always become complex for negative x . Even though there are no real solutions for negative x to equation (2.36), the last term can become arbitrarily small for very small a leading to a significantly enhanced dislocation field close to the dotted line (which is the solution at $a = 0$) even for negative x . This, of course, is expected since the general solution must tend to the constant velocity solution as $a \rightarrow 0$, see also Fig. 3.

see the denominators in Eq. (2.25). Real solutions $y(x)$ can only be expected for $\eta' v_{\text{crit}} \leq 1$, and in proximity to the dislocation core this is the case when the dislocation velocity $v(t)$ approaches v_{crit} . It will be convenient to shift $x \rightarrow x + at^2/2$ so that $x = 0 = y$ is the current position of the dislocation core. Consider now $\tau = t - (x + at^2/2)\eta'$, $t = v_{\text{crit}}/a$, and $\eta'^2 = 1/|2ax + v_{\text{crit}}^2|$. Close to the core, where the product $2a|x| < v_{\text{crit}}^2$, we may drop the absolute value in η' . Hence, dividing the whole equation above by η'^2 we presently have

$$\begin{aligned}
 0 &= \left[\frac{v_{\text{crit}}}{a\eta'} - \left(2x + \frac{v_{\text{crit}}^2}{a} \right) + y \frac{\tilde{B}}{2\tilde{C}} \right]^2 + \left(1 - \frac{1}{v_{\text{crit}}^2 \eta'^2} \right) \frac{y^2}{\tilde{C}} \left(1 - \frac{\tilde{B}}{4\tilde{C}} \right) \\
 &= \left[\frac{v_{\text{crit}}}{a} \sqrt{2ax + v_{\text{crit}}^2} - \frac{1}{a} (2ax + v_{\text{crit}}^2) + y \frac{\tilde{B}}{2\tilde{C}} \right]^2 - \frac{2ax}{v_{\text{crit}}^2} \frac{y^2}{\tilde{C}} \left(1 - \frac{\tilde{B}}{4\tilde{C}} \right), \quad (2.36)
 \end{aligned}$$

which is a quadratic equation for $y(x)$ with real solutions only for positive x . Typically, critical velocities are of the order of a few km/s and Burgers vector length scales are a few Ångström. Therefore, if $v_{\text{crit}} \sim 10^3 \text{ m/s}$ and $x < 10^{-9} \text{ m}$ near the core, $2ax < v_{\text{crit}}^2$ implies $a < 10^{15} \text{ m/s}^2$ as an upper limit for dropping the absolute value in η'^2 leading to (2.36). Figure 2 illustrates the solutions to this equation for two different values of a as well as for $a = 0$ (which is the only case where a real solution exists for $x < 0$). In the isotropic limit, $\tilde{B} \rightarrow 0$ (see Section 2.4 below), and the contours become $y(x) \approx \frac{xv_{\text{crit}}^2}{2a} + \mathcal{O}(x^2) \ll 1$ for positive x and $a \neq 0$, and $x = 0$ for any a (including zero).

Markenscoff et al. [22] argue that independent of $\eta(x)$, the singularities in the dislocation field are only removed once the core itself is regularized (i.e. modeled to be of finite size) in some fashion;

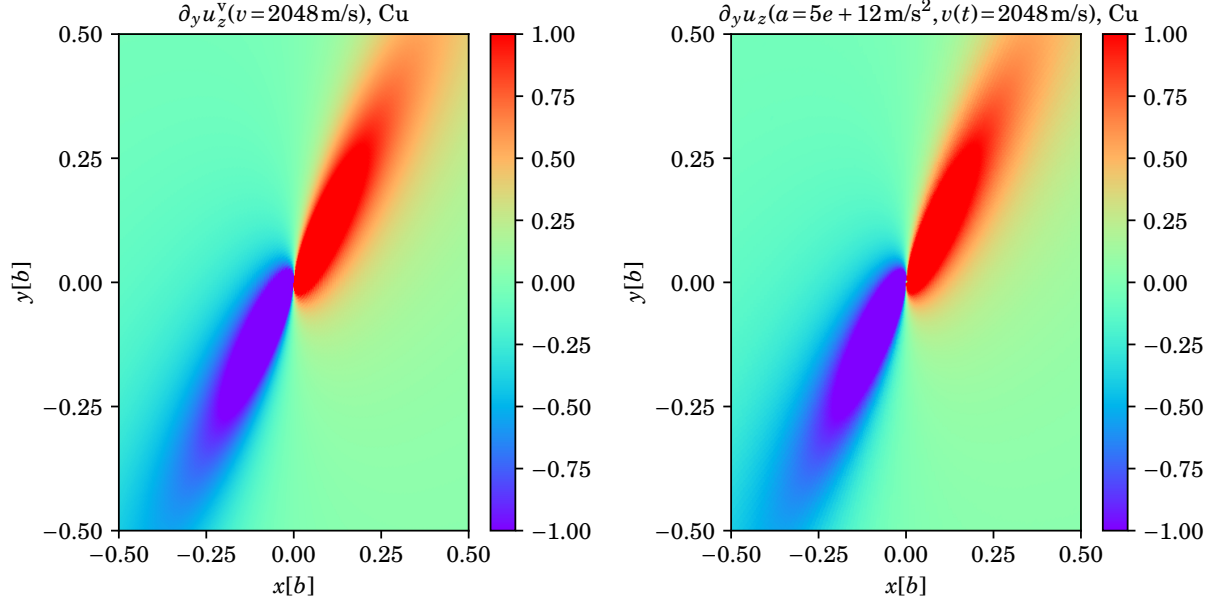


Figure 3: We show $\partial_y u_z$ at dislocation velocity $v = 2.05\text{km/s}$ for fcc copper ($\rho = 8.96\text{g/ccm}$, $b = 2.56\text{\AA}$, $c_{44} = 75.7\text{GPa}$, and $c' = 23.55\text{GPa}$, see [20, 44]). This velocity corresponds to roughly 93% of the critical velocity and coincides with the lowest shear wave speed propagating in the direction of v , and as argued in Ref. [20], nothing special happens at this velocity. Both plots are centered at the dislocation core, showing the plane perpendicular to the dislocation line in units of a Burgers vector. On the left, we show the steady state-solution (2.31b) and on the right we show the full solution for constant acceleration (2.25b) with (2.28) and $a = 5 \times 10^{12}\text{m/s}^2$ at time $t_v = v/a = 4.1 \times 10^{-10}\text{s}$ needed to reach velocity v . At this point, the dislocation has traveled a distance of 0.42 microns. The integration w.r.t. x' in the full solution as well as the subsequent time derivative have been carried out numerically, though we point out that the \mathcal{F} dependent terms are much smaller compared to the others and the figure on the right does not change visibly if those terms are neglected. We see that the changes in the dislocation displacement gradient due to the inclusion of acceleration are barely visible in this example.

see also [45, 46] for a discussion of the wave-front asymptotics in the isotropic limit. Similarly, the author of Ref. [31] shows that a regularized core can remove the singularity in the anisotropic steady-state special case, see (2.31).

Another point to note is that for small accelerations a , the \mathcal{F} dependent terms are small compared to the others (and vanish identically for constant velocity as seen in the previous subsection), and these terms become important only when dislocations accelerate quickly. In dislocation dynamics where, according to MD simulations, dislocations reach their steady state velocity within picoseconds (see e.g. [20]), “small” accelerations can still mean of the order of $a \sim 10^{12}\text{m/s}^2$.

Figure 3 shows an example of a screw dislocation in copper moving at about 93% v_{crit} , once for the steady state solution (2.31), and once for the full solution (2.25b) with constant acceleration $a = 5 \times 10^{12}\text{m/s}^2$, see (2.28). The acceleration a was chosen at a typical peak value according to single crystal plasticity simulations [47] and high enough such that the dislocation can easily achieve its target velocity by traveling less than a micron, i.e. in a fraction of even the smallest single crystal grains within a polycrystal. Furthermore, “low” dislocation densities within a single crystal are considered to be of the order of 10^6mm^{-2} which means the mean free path of an accelerating dislocation will then also be of the order of one micron [12, 48].

We see that, indeed as expected, the dislocation field of a moderately accelerated screw dislocation at any given time-snapshot does not look too different from the steady state solution (2.31) at the same velocity. Edge and mixed dislocations have yet to be studied within the present framework before we can generalize this statement. In a real crystal we cannot expect a to be constant, but rather it will initially be large and then tend to zero as the dislocation approaches its steady state velocity (if it has not encountered an obstacle before that time).

Due to the divergence at $v(t) = v_{\text{crit}}$ within (2.25), the transition to supersonic speeds will depend on how the dislocation core is modeled, since the remaining divergence at the critical velocity can only be expected to be removed by an extended core [22, 31]. While Ref. [22] studied a ramp-like core to regularize the divergence only in the isotropic limit and Ref. [31] studied an elliptic core in the anisotropic steady-state limit, there is no immediate reason why these strategies should not work also in the present general anisotropic case. This, however, is beyond the scope of the present work and is left for future studies.

2.4 The isotropic limit

In the isotropic limit, $c_{11} = c_{12} + 2c_{44}$ which leads to $\tilde{B} = 0$, $\tilde{C} = C/A = 1$, and $c_A = c_T = \sqrt{c_{44}/\rho}$ is the transverse sound speed. Furthermore, $p_0 = \frac{x}{rc_T}$. The general solution (2.25) then simplifies to

$$\begin{aligned} \partial_x u_z^{\text{iso}}(x, y, t) = & \frac{b}{2\pi} \partial_t \int_0^\infty dx' \left(\mathcal{F}_x[\eta(x'), \tilde{t}, t] - \mathcal{F}_x[\eta(x) + (x' - x)\eta'(x), \tilde{t}, t] \right) \Big|_{\tilde{t}=t} \\ & + \frac{b}{2\pi} \frac{y}{r^2} \left[\frac{\Theta\left(t - \frac{r}{c_T}\right)}{\sqrt{1 - \frac{r^2}{t^2 c_T^2}}} + \frac{\Theta\left(\tau - \frac{r}{c_T}\right) \left(\tau x \eta'(x) \left[2 - \frac{r^2}{\tau^2 c_T^2} \right] - \left[\tau^2 - \frac{y^2}{c_T^2} \right] \right)}{\sqrt{1 - \frac{r^2}{\tau^2 c_T^2} \left(\tau^2 - \frac{y^2}{c_T^2} - 2\tau x \eta'(x) + (\eta'(x))^2 r^2 \right)}} \right] \\ & + \frac{b \operatorname{sgn}(y)}{2} \operatorname{sgn}(-x) \eta'(x) \Theta\left(\frac{x}{rc_T} - \eta'(x)\right) \delta\left(t - x\eta'(x) - |y| \sqrt{\frac{1}{c_T^2} - (\eta'(x))^2}\right), \quad (2.37a) \end{aligned}$$

$$\begin{aligned} \partial_y u_z^{\text{iso}}(x, y, t) = & \frac{b}{2\pi} \partial_t \int_0^\infty dx' \left(\mathcal{F}_y[\eta(x'), \tilde{t}, t] - \mathcal{F}_y[\eta(x) + (x' - x)\eta'(x), \tilde{t}, t] \right) \Big|_{\tilde{t}=t} + \frac{b \operatorname{sgn}(-x)}{2c_T} \delta\left(t - \frac{|y|}{c_T}\right) \\ & + \frac{b}{2\pi} \frac{1}{r^2} \left\{ \Theta\left(t - \frac{r}{c_T}\right) + \Theta\left(\tau - \frac{r}{c_T}\right) \frac{\tau \eta'(x) (y^2 - x^2) + x \left(\frac{x \eta'(x)}{\tau} - 1 \right) \frac{r^2}{c_T^2} + x \left(\tau^2 - \frac{y^2}{c_T^2} \right)}{\sqrt{1 - \frac{r^2}{\tau^2 c_T^2} \left(\tau^2 - \frac{y^2}{c_T^2} - 2\tau x \eta'(x) + (\eta'(x))^2 r^2 \right)}} \right\} \\ & + \frac{b}{2} \operatorname{sgn}(-x) \Theta\left(\frac{x}{rc_T} - \eta'(x)\right) \sqrt{\frac{1}{c_T^2} - (\eta'(x))^2} \delta\left(t - x\eta'(x) - |y| \sqrt{\frac{1}{c_T^2} - (\eta'(x))^2}\right), \quad (2.37b) \end{aligned}$$

with

$$\mathcal{F}_x[\eta] = \Theta\left(\tilde{t} - \eta - \frac{r'}{c_T}\right) \frac{y(x - x') \left(2(t - \eta)^2 - \frac{r'^2}{c_T^2} \right)}{r'^4 \sqrt{(t - \eta)^2 - \frac{r'^2}{c_T^2}}}, \quad (2.38a)$$

$$\mathcal{F}_y[\eta] = \Theta\left(\tilde{t} - \eta - \frac{r'}{c_T}\right) \frac{1}{r'^4} \left[\frac{y^2(t-\eta)^2}{\sqrt{(t-\eta)^2 - \frac{r'^2}{c_T^2}}} - (x-x')^2 \sqrt{(t-\eta)^2 - \frac{r'^2}{c_T^2}} \right], \quad (2.38b)$$

and

$$r^2 = (x^2 + y^2), \quad r'^2 = ((x-x')^2 + y^2), \quad \tau = t - (\eta(x) - x\eta'(x)). \quad (2.39)$$

The special case of constant velocity, using relations (2.28) yields

$$\begin{aligned} \partial_x u_z^{v,\text{iso}}(x, y, t) &= \frac{b}{2\pi} \Theta\left(t - \frac{r}{c_T}\right) \frac{y\left(1 - x\frac{v}{tc_T^2}\right)}{\sqrt{1 - \frac{r^2}{t^2 c_T^2}} \left((x-vt)^2 + y^2\left(1 - \frac{v^2}{c_T^2}\right)\right)} \\ &\quad + \frac{b \operatorname{sgn}(y)}{2} \operatorname{sgn}(-x) \Theta\left(\frac{x}{rc_T} - \frac{1}{v}\right) \delta\left(x - vt + |y| \sqrt{\frac{v^2}{c_T^2} - 1}\right), \end{aligned} \quad (2.40a)$$

$$\begin{aligned} \partial_y u_z^{v,\text{iso}}(x, y, t) &= \frac{b}{2\pi} \frac{\Theta\left(t - \frac{r}{c_T}\right)}{\sqrt{1 - \frac{r^2}{t^2 c_T^2}} \left((x-vt)^2 + y^2\left(1 - \frac{v^2}{c_T^2}\right)\right)} \left\{ \frac{x(r^2 - 2vtx)}{c_T^2 \left(t^2 - \frac{y^2}{c_T^2}\right)} - (x-vt) + \frac{vx^2}{tc_T^2} \right\} \\ &\quad + \frac{b \operatorname{sgn}(-x)}{2c_T} \delta\left(t - \frac{|y|}{c_T}\right) + \frac{b}{2} \operatorname{sgn}(-x) \left(\sqrt{\frac{v^2}{c_T^2} - 1} \right) \Theta\left(\frac{x}{rc_T} - \frac{1}{v}\right) \delta\left(x - vt + |y| \sqrt{\frac{v^2}{c_T^2} - 1}\right), \end{aligned} \quad (2.40b)$$

which generalizes (and corrects⁵) the earlier result of Ref. [37, Eq. (16)] for $\partial_y u_z^v(x, y, t)$ to all velocities including the supersonic regime. As before, the steady-state solution follows by taking the large time limit while keeping $x' := x - vt$ at a fixed value:

$$\begin{aligned} \lim_{t \rightarrow \infty} \partial_{x'} u_z^{v,\text{iso}}(x(x', t), y, t) &= \frac{b}{2\pi} \frac{y \Theta(1 - |\beta|)}{(x')^2 \gamma_T + y^2 / \gamma_T} - \frac{b \operatorname{sgn}(y)}{2} \delta\left(x' + |y| \sqrt{\beta^2 - 1}\right), \\ \lim_{t \rightarrow \infty} \partial_y u_z^{v,\text{iso}}(x(x', t), y, t) &= \frac{b}{2\pi} \frac{-x' \Theta(1 - |\beta|)}{(x')^2 \gamma_T + y^2 / \gamma_T} - \frac{b}{2} \left(\sqrt{\beta^2 - 1} \right) \delta\left(x' + |y| \sqrt{\beta^2 - 1}\right), \end{aligned} \quad (2.41)$$

where $\gamma_T^2 = 1/(1 - \beta_T^2)$ and $\beta_T = v/c_T$, and the argument of the step function in the first term tends to $\pm\infty$ depending on whether v is smaller or larger than the transverse sound speed. In the subsonic regime, $v < c_T$, the delta functions are identically zero and these expressions indeed coincide with the well-known steady-state solution of Eshelby [13, 49] for screw dislocations moving subsonically. On the other hand, in the supersonic regime, $v > c_T$, the step function is zero leaving only the delta functions as the supersonic solution, consistent with the discussion in Ref. [13, Sec. 4.2].

⁵ Indeed, there were two issues with the earlier result of Ref. [37, Eq. (16)]: The first term in (2.10) (which is independent of η) was erroneously identified with the static limit and replaced by that known result. This later prevented the combination and simplification of terms in the final result. Additionally, Ref. [37, Eq. (16)] contains an incorrect last term, likely due to an algebraic error, and therefore fails to reproduce the well-known steady-state solution of Eshelby [13, 49] in the large time limit.

3 Conclusion

In this paper, we have derived the most general solution for an accelerating pure screw dislocation in an anisotropic crystal. The term ‘pure’ screw entails an important restriction: Unless the slip system exhibits a ‘reflection’ symmetry, screw and edge dislocations mix and cannot be separated. Hence, the present solution applies only to reflection symmetric slip systems, such as all 12 fcc slip systems and a number of hcp slip systems, but none of the 48 bcc slip systems.

We confirm for the anisotropic case what Markenscoff et al. have concluded some time ago for the isotropic limit only: that the divergence at a ‘critical’ dislocation velocity (which separates the subsonic from the supersonic regime), persists for general accelerating dislocations with vanishing core size [22]. In other words, the remaining singularities (including at the core) must be removed by regularizing the core in an appropriate fashion [50]. Recent work on modeling dislocation cores (from theory) in a realistic way can be found in [31, 51–54] and references therein. Furthermore, we saw that when simulating dislocations in larger codes, the computationally less expensive steady state solution (2.31) can be expected to be a fairly good approximation for subsonic screw dislocations with low to moderate acceleration compared to its more general counterpart (and our main result) Eq. (2.25). The general solution Eq. (2.25) has been derived for the first time within this work, and will also be an important starting point when studying potential transitions to supersonic speeds within future work. The latter will depend on how the dislocation core is modeled (which is beyond the scope of this work), and will thus generalize to accelerating dislocations what has been done in Ref. [31] for the steady-state limit.

Finally, we showed how various limits reduce to known results: the isotropic limit as well as steady-state solutions for both subsonic and supersonic regimes are recovered from our general result which itself applies to any time-dependent velocity $v(t) \neq v_{\text{crit}}$, as long as it does not exactly coincide with the critical velocity (which in turn is higher than the lowest shear wave speed for fcc screw dislocations [20]).

Acknowledgements

The author would like to thank B. A. Szajewski, S. Fensin, D. J. Luscher, R. G. Hoagland, and J. Chen for related discussions. This work was mostly supported by the Institute for Material Science at Los Alamos National Laboratory. In particular, the author acknowledges support by the IMS Rapid Response program. Furthermore, the author is grateful for the support of the Materials project within the Advanced Simulation and Computing, Physics and Engineering Models Program of the U.S. Department of Energy under contract 89233218CNA000001 in the final stages of this work.

A Rotation matrix and coefficients of the differential equation

In this short appendix we review how to derive the coefficients A , B , and C of the differential equation (2.3) for a given slip system at the example of fcc metals with Burgers unit vector $\hat{b} = (1, 1, 0)/\sqrt{2}$ and slip plane normal $\hat{n}_0 = (1, -1, 1)/\sqrt{3}$ in Cartesian coordinates. For a screw dislocation, the line sense is parallel (or antiparallel) to \hat{b} , so from $\hat{t}(\vartheta) = \frac{1}{b} [\vec{b} \cos \vartheta + \vec{b} \times \hat{n}_0 \sin \vartheta]$ with character angle $\vartheta = 0$ we presently have $\hat{t}(0) = \hat{b} = \frac{1}{b} \vec{b}$. Assuming a straight dislocation that is much longer than its Burgers vector length, the only velocity component that matters is the one perpendicular to the dislocation line, i.e. $\vec{v} = \pm v \hat{v}$ and $\hat{v} = \hat{n}_0 \times \hat{t}(0) = \hat{n}_0 \times \hat{b} = (-1, 1, 2)/\sqrt{6}$. In order to derive A , B , and C of the differential equation, we need the rotation matrix that aligns $\hat{b} \parallel \hat{z}$, $\hat{n}_0 \parallel \hat{y}$, and $\hat{v} \parallel \hat{x}$. Given a

rotation axis unit vector \hat{a} and an angle ϕ , the rotation matrix is

$$U(\hat{a}, \phi)_{ij} = \delta_{ij} + \sin(\phi)\epsilon_{ijk}\hat{a}_k + (1 - \cos(\phi))\epsilon_{ilk}\hat{a}_k\epsilon_{ljm}\hat{a}_m, \quad (\text{A.1})$$

according to Rodrigues formula. In order to align $\hat{n}_0 \parallel \hat{y}$, one needs to rotate around rotation axis $\vec{a}_0 = \hat{y} \times \hat{n}_0$ by an angle $\cos(\phi_0) = (\hat{y} \cdot \hat{n}_0)$ (with $\sin(\phi_0) = |a_0|$) so that $\hat{a}_0 = \vec{a}_0 / \sin(\phi_0)$. Then, in a second step one must rotate around axis $\vec{a}_1 = \hat{z} \times (U_0 \cdot \hat{b})$ with angle $\cos(\phi_1) = \hat{z} \cdot (U_0 \cdot \hat{b})$, resp. $\sin(\phi_1) = |\vec{a}_1|$ using the same procedure. For our present slip system we find [20]

$$U = U_1 \cdot U_0 = \frac{1}{\sqrt{6}} \begin{pmatrix} -1 & 1 & 2 \\ \sqrt{2} & -\sqrt{2} & \sqrt{2} \\ \sqrt{3} & \sqrt{3} & 0 \end{pmatrix} = \begin{pmatrix} \hat{v}^T \\ \hat{n}_0^T \\ \hat{b}^T \end{pmatrix},$$

$$U \cdot \hat{b} = \hat{z}, \quad U \cdot \hat{n}_0 = \hat{y}, \quad U \cdot \hat{v} = \hat{x}. \quad (\text{A.2})$$

This rotation matrix is then used to rotate the tensor of second order elastic constants (2.2) into the dislocation reference frame, i.e.:

$$C'_{ijkl} = U_{ii'}U_{jj'}U_{kk'}U_{ll'}C_{i'j'k'l'}. \quad (\text{A.3})$$

Using these elastic constants to compute the stress tensor from the ansatz $\vec{u} = (0, 0, u_z(x, y, t))$ for the displacement field of a pure screw dislocation, we easily verify that the only non-vanishing stress components are $\sigma_{13} = \sigma_{31} = \frac{1}{3}(c' + 2c_{44})u_{z,x} + \frac{\sqrt{2}}{3}(c_{44} - c')u_{z,y}$ and $\sigma_{23} = \sigma_{32} = \frac{\sqrt{2}}{3}(c_{44} - c')u_{z,x} + \frac{1}{3}(c_{44} + 2c')u_{z,y}$ with $c' = (c_{11} - c_{12})/2$. Since $\sigma_{xx} = \sigma_{xy} = \sigma_{yy} = 0$, the present slip system fulfills the symmetry requirements allowing us to study pure screw dislocations. The divergence of this stress tensor straightforwardly computes to $\partial_i \sigma_{ij} = (0, 0, A\partial_x^2 u_z + B\partial_x \partial_y u_z + C\partial_y^2 u_z)$ with coefficients

$$A = \frac{1}{3}(c' + 2c_{44}), \quad B = \frac{2\sqrt{2}}{3}(c_{44} - c'), \quad C = \frac{1}{3}(c_{44} + 2c'). \quad (\text{A.4})$$

One may repeat this exercise for the other 11 fcc slip systems to check that indeed all of them yield the same coefficients above.

Let us check condition $\tilde{B}^2 < 4\tilde{C}$, resp. $B^2 < 4AC$ (see Eq. (2.9)) for the fcc slip systems: A and C are weighted averages of the two shear moduli with $A > C$ for Zener ratio $Z := c_{44}/c' > 1$ and $A < C$ for $Z < 1$. B , on the other hand, is given by the difference of the two shear moduli and is positive for $Z > 1$ and negative for $Z < 1$. Plugging (A.4) into the above condition yields

$$4AC - B^2 = 4c_{44}c' > 0, \quad (\text{A.5})$$

which is clearly fulfilled for all Zener ratios. Also notice that both $A > 0$ and $C > 0$, whereas B can be positive or negative depending on the Zener ratio. Our rescaled coefficients finally are $\tilde{B} = B/A = 2\sqrt{2}(c_{44} - c')/(c' + 2c_{44}) = 2\sqrt{2}(Z - 1)/(1 + 2Z)$ and $\tilde{C} = C/A = (2c' + c_{44})/(c' + 2c_{44}) = (2 + Z)/(1 + 2Z)$. In the isotropic limit, $Z \rightarrow 1$ and hence $\tilde{B} \rightarrow 0$ and $\tilde{C} \rightarrow 1$.

B Useful relations

We list some relations needed in the derivation of our main result in Section 2 above:

$$dp_{\pm}p_{\pm} = \frac{\tau d\tau}{R^4} \left(x - y \frac{\tilde{B}}{2\tilde{C}} \pm i \frac{|y| \frac{1}{\tilde{C}} \left(1 - \frac{\tilde{B}^2}{4\tilde{C}} \right)}{\sqrt{\frac{1}{\tilde{C}} \left(1 - \frac{\tilde{B}^2}{4\tilde{C}} \right) - \frac{R^2}{\tau^2 c_A^2 \tilde{C}}}} \right) \left(\left(x - y \frac{\tilde{B}}{2\tilde{C}} \right) \pm i |y| \sqrt{\frac{1}{\tilde{C}} \left(1 - \frac{\tilde{B}^2}{4\tilde{C}} \right) - \frac{R^2}{\tau^2 c_A^2 \tilde{C}}} \right), \quad (\text{B.1})$$

$$\Im(dp_{+}p_{+}) = \frac{-i}{2}(dp_{+}p_{+} - dp_{-}p_{-}) = \frac{\tau d\tau}{R^4} \left(x - y \frac{\tilde{B}}{2\tilde{C}} \right) \frac{|y|}{\tilde{C}} \left[\frac{2 \left(1 - \frac{\tilde{B}^2}{4\tilde{C}} \right) - \frac{R^2}{\tau^2 c_A^2 \tilde{C}}}{\sqrt{\frac{1}{\tilde{C}} \left(1 - \frac{\tilde{B}^2}{4\tilde{C}} \right) - \frac{R^2}{\tau^2 c_A^2 \tilde{C}}}} \right], \quad (\text{B.2})$$

$$dp_{\pm}\beta_{\pm} = \frac{\tau d\tau}{R^4} \left[\left(\frac{|y|}{\tilde{C}} - x \frac{\text{sgn}(y)\tilde{B}}{2\tilde{C}} \right) \mp ix \sqrt{\frac{1}{\tilde{C}} \left(1 - \frac{\tilde{B}^2}{4\tilde{C}} \right) - \frac{R^2}{\tau^2 c_A^2 \tilde{C}}} \right] \left(x - y \frac{\tilde{B}}{2\tilde{C}} \pm i \frac{\frac{|y|}{\tilde{C}} \left(1 - \frac{\tilde{B}^2}{4\tilde{C}} \right)}{\sqrt{\frac{1}{\tilde{C}} \left(1 - \frac{\tilde{B}^2}{4\tilde{C}} \right) - \frac{R^2}{\tau^2 c_A^2 \tilde{C}}}} \right), \quad (\text{B.3})$$

$$\begin{aligned} \Im(dp_{+}\beta_{+}) &= \frac{-i}{2}(dp_{+}\beta_{+} - dp_{-}\beta_{-}) = \frac{\tau d\tau}{R^4} \left[\frac{\frac{1}{\tilde{C}} \left(\frac{y^2}{\tilde{C}} - x \frac{y\tilde{B}}{2\tilde{C}} \right) \left(1 - \frac{\tilde{B}^2}{4\tilde{C}} \right) - x \left(x - y \frac{\tilde{B}}{2\tilde{C}} \right) \left(\frac{1}{\tilde{C}} \left(1 - \frac{\tilde{B}^2}{4\tilde{C}} \right) - \frac{R^2}{\tau^2 c_A^2 \tilde{C}} \right)}{\sqrt{\frac{1}{\tilde{C}} \left(1 - \frac{\tilde{B}^2}{4\tilde{C}} \right) - \frac{R^2}{\tau^2 c_A^2 \tilde{C}}}} \right] \\ &= \frac{\tau d\tau}{R^4 \tilde{C}} \left[\frac{\left(\frac{y^2}{\tilde{C}} - x^2 \right) \left(1 - \frac{\tilde{B}^2}{4\tilde{C}} \right) + x \left(x - y \frac{\tilde{B}}{2\tilde{C}} \right) \frac{R^2}{\tau^2 c_A^2 \tilde{C}}}{\sqrt{\frac{1}{\tilde{C}} \left(1 - \frac{\tilde{B}^2}{4\tilde{C}} \right) - \frac{R^2}{\tau^2 c_A^2 \tilde{C}}}} \right], \end{aligned} \quad (\text{B.4})$$

$$\beta_{+}p_{-} = \frac{1}{|y|} (\tau p_{-} - |p|^2 x), \quad (\text{B.5})$$

$$\begin{aligned} \Im(dp_{+}\beta_{+}p_{-}) &= \frac{1}{|y|} (\tau \Im(dp_{+}p_{-}) - |p|^2 x \Im(dp_{+})) \\ &= \frac{d\tau}{R^2 \tilde{C} \sqrt{\frac{1}{\tilde{C}} \left(1 - \frac{\tilde{B}^2}{4\tilde{C}} \right) - \frac{R^2}{\tau^2 c_A^2 \tilde{C}}}} \left[\frac{1}{c_A^2} \left(x - y \frac{\tilde{B}}{2\tilde{C}} \right) - \frac{x}{R^2} \left(\tau^2 - \frac{y^2}{c_A^2 \tilde{C}} \right) \left(1 - \frac{\tilde{B}^2}{4\tilde{C}} \right) \right], \end{aligned} \quad (\text{B.6})$$

and the primed counterparts of these expressions follow from $x \rightarrow (x - x')$. We also need

$$\begin{aligned} |p|^2 &= p_{+}p_{-} = \frac{1}{R^2} \left(\tau^2 - \frac{y^2}{c_A^2 \tilde{C}} \right), \\ |\eta'(x) - p|^2 &= \frac{1}{R^2} \left(\tau^2 - \frac{y^2}{c_A^2 \tilde{C}} - 2\tau \eta'(x) \left(x - y \frac{\tilde{B}}{2\tilde{C}} \right) + (\eta'(x))^2 R^2 \right). \end{aligned} \quad (\text{B.7})$$

In the isotropic limit, the following simplifications apply because of $\tilde{B} \rightarrow 0$, $\tilde{C} \rightarrow 1$, $c_A \rightarrow c_T$:

$$\begin{aligned} p_{\pm} &\rightarrow \frac{1}{r^2} \left(x\tau \pm i|y|\sqrt{\tau^2 - r^2/c_T^2} \right), & \beta_{\pm} &\rightarrow \frac{1}{r^2} \left(|y|\tau \mp ix\sqrt{\tau^2 - r^2/c_T^2} \right), \\ dp_{\pm} &\rightarrow \frac{\pm i\beta_{\pm}d\tau}{\sqrt{\tau^2 - r^2/c_T^2}}, & R^2 &\rightarrow r^2 = x^2 + y^2. \end{aligned} \quad (\text{B.8})$$

References

- [1] B. L. Hansen, I. J. Beyerlein, C. A. Bronkhorst, E. K. Cerreta, and D. Dennis-Koller, “A dislocation-based multi-rate single crystal plasticity model”, *Int. J. Plast.* **44** (2013) 129–146.
- [2] D. J. Luscher, J. R. Mayeur, H. M. Mourad, A. Hunter, and M. A. Kenamond, “Coupling continuum dislocation transport with crystal plasticity for application to shock loading conditions”, *Int. J. Plast.* **76** (2016) 111–129.
- [3] E. M. Nadgornyi, “Dislocation dynamics and mechanical properties of crystals”, *Prog. Mater. Sci.* **31** (1988) 1–530.
- [4] V. I. Alshits, “The phonon-dislocation interaction and its role in dislocation dragging and thermal resistivity”, in *Elastic Strain Fields and Dislocation Mobility*, V. L. Indenbom and J. Lothe, eds., vol. 31 of *Modern Problems in Condensed Matter Sciences*, pp. 625–697, (Elsevier, 1992).
- [5] D. N. Blaschke, E. Mottola, and D. L. Preston, “Dislocation drag from phonon wind in an isotropic crystal at large velocities”, *Phil. Mag.* **100** (2020) 571–600, [arXiv:1907.00101 \[cond-mat.mtrl-sci\]](#).
- [6] D. N. Blaschke, “Velocity dependent dislocation drag from phonon wind and crystal geometry”, *J. Phys. Chem. Solids* **124** (2019) 24–35, [arXiv:1804.01586 \[cond-mat.mtrl-sci\]](#).
- [7] H. M. Zbib, M. Rhee, and J. P. Hirth, “On plastic deformation and the dynamics of 3D dislocations”, *Int. J. Mech. Sci.* **40** (1998) 113–127.
- [8] N. M. Ghoniem, S.-H. Tong, and L. Z. Sun, “Parametric dislocation dynamics: A thermodynamics-based approach to investigations of mesoscopic plastic deformation”, *Phys. Rev.* **B61** (2000) 913–927.
- [9] N. Bertin, M. V. Upadhyay, C. Pradalier, and L. Capolungo, “A FFT-based formulation for efficient mechanical fields computation in isotropic and anisotropic periodic discrete dislocation dynamics”, *Mod. Sim. Mater. Sci. Eng.* **23** (2015) 065009.
- [10] Y. Cui, G. Po, Y.-P. Pellegrini, M. Lazar, and N. Ghoniem, “Computational 3-dimensional dislocation elastodynamics”, *J. Mech. Phys. Solids* **126** (2019) 20–51.
- [11] J. T. Lloyd, J. D. Clayton, R. A. Austin, and D. L. McDowell, “Plane wave simulation of elastic-viscoplastic single crystals”, *J. Mech. Phys. Solids* **69** (2014) 14–32.
- [12] D. N. Blaschke, A. Hunter, and D. L. Preston, “Analytic model of the remobilization of pinned glide dislocations: including dislocation drag from phonon wind”, *Int. J. Plast.* **131** (2020) 102750, [arXiv:1912.08851 \[cond-mat.mtrl-sci\]](#).
- [13] J. Weertman and J. R. Weertman, “Moving dislocations”, in *Moving Dislocations*, F. R. N. Nabarro, ed., vol. 3 of *Dislocations in Solids*, pp. 1–59, (Amsterdam: North Holland Pub. Co., 1980).
- [14] V. Nosenko, S. Zhdanov, and G. Morfill, “Supersonic dislocations observed in a plasma crystal”, *Phys. Rev. Lett.* **99** (2007) 025002, [arXiv:0709.1782 \[cond-mat.soft\]](#).
- [15] D. L. Olmsted, L. G. Hector Jr., W. A. Curtin, and R. J. Clifton, “Atomistic simulations of dislocation mobility in Al, Ni and Al/Mg alloys”, *Mod. Simul. Mater. Sci. Eng.* **13** (2005) 371, [arXiv:cond-mat/0412324](#).
- [16] J. Marian and A. Caro, “Moving dislocations in disordered alloys: Connecting continuum and discrete models with atomistic simulations”, *Phys. Rev.* **B74** (2006) 024113.
- [17] H. Tsuzuki, P. S. Branicio, and J. P. Rino, “Accelerating dislocations to transonic and supersonic speeds in anisotropic metals”, *Appl. Phys. Lett.* **92** (2008) 191909.

- [18] E. Oren, E. Yahel, and G. Makov, “Dislocation kinematics: a molecular dynamics study in Cu”, *Mod. Simul. Mater. Sci. Eng.* **25** (2017) 025002.
- [19] S. Peng, Y. Wei, Z. Jin, and W. Yang, “Supersonic screw dislocations gliding at the shear wave speed”, *Phys. Rev. Lett.* **122** (2019) 045501.
- [20] D. N. Blaschke, J. Chen, S. Fensin, and B. Szajewski, “Common misconceptions about ‘transonic’ screw dislocations”, [arXiv:2008.13760](#) [`cond-mat.mtrl-sci`].
- [21] P. Rosakis, “Supersonic dislocation kinetics from an augmented Peierls model”, *Phys. Rev. Lett.* **86** (2001) 95–98.
- [22] X. Markenscoff and S. Huang, “Analysis for a screw dislocation accelerating through the shear-wave speed barrier”, *J. Mech. Phys. Solids* **56** (2008) 2225–2239.
- [23] X. Markenscoff and S. Huang, “The energetics of dislocations accelerating and decelerating through the shear-wave speed barrier”, *Appl. Phys. Lett.* **94** (2009) 021906.
- [24] S. Huang and X. Markenscoff, “Is intersonic dislocation motion possible? Singularity analysis for an edge dislocation accelerating through the shear wave speed barrier”, *Exp. Mech.* **49** (2009) 219–224.
- [25] L. Pilon, C. Denoual, and Y.-P. Pellegrini, “Equation of motion for dislocations with inertial effects”, *Phys. Rev.* **B76** (2007) 224105.
- [26] Y.-P. Pellegrini, “Dynamic Peierls-Nabarro equations for elastically isotropic crystals”, *Phys. Rev.* **B81** (2010) 024101, [arXiv:0908.2371](#) [`cond-mat.mtrl-sci`].
- [27] Y.-P. Pellegrini, “Equation of motion and subsonic-transonic transitions of rectilinear edge dislocations: A collective-variable approach”, *Phys. Rev.* **B90** (2014) 054120, [arXiv:1307.5244](#) [`cond-mat.mtrl-sci`].
- [28] Y.-P. Pellegrini, “Dynamic Peach-Koehler self-force, inertia, and radiation damping of a regularized dislocation”, [arXiv:2005.12704](#) [`cond-mat.mtrl-sci`].
- [29] D. J. Bacon, D. M. Barnett, and R. O. Scattergood, “Anisotropic continuum theory of lattice defects”, *Prog. Mater. Sci.* **23** (1980) 51–262.
- [30] Y.-P. Pellegrini, “Causal Stroh formalism for uniformly-moving dislocations in anisotropic media: Somigliana dislocations and Mach cones”, *Wave Motion* **68** (2017) 128–148, [arXiv:1609.02749](#) [`cond-mat.mtrl-sci`].
- [31] Y.-P. Pellegrini, “Uniformly-moving non-singular dislocations with ellipsoidal core shape in anisotropic media”, *J. Micromech. Molec. Phys.* **3** (2018) 1840004, [arXiv:1808.10272](#) [`physics.class-ph`].
- [32] B. Gurrutxaga-Lerma, J. Verschueren, A. P. Sutton, and D. Dini, “The mechanics and physics of high-speed dislocations: a critical review”, *Int. Mater. Rev.* (2020) in press.
- [33] J. P. Hirth and J. Lothe, *Theory of Dislocations*, second ed., (New York: Wiley, 1982).
- [34] L. Cagniard, *Réflexion et réfraction des ondes séismiques progressives*. PhD thesis, Université de Paris, Sorbonne, 1939.
- [35] A. T. De Hoop, “A modification of Cagniard’s method for solving seismic pulse problems”, *Appl. Sci. Res.* **8** (1960) 349–356.
- [36] L. B. Freund, “The response of an elastic solid to nonuniformly moving surface loads”, *J. Appl. Mech.* **40** (1973) 699–704.
- [37] X. Markenscoff, “The transient motion of a nonuniformly moving dislocation”, *J. Elast.* **10** (1980) 193–201.
- [38] M. Mitra, “Surface displacement produced by an underground fracture”, *Geophysics* **31** (1966) 204–213.
- [39] D. M. Boore, K. Aki, and T. Todd, “A two-dimensional moving dislocation model for a strike-slip fault”, *Bull. Seismol. Soc. Am.* **61** (1971) 177–194.
- [40] D. M. Boore and M. D. Zoback, “Near-field motions from kinematic models of propagating faults”, *Bull. Seismol. Soc. Am.* **64** (1974) 321–342.

- [41] R. Madariaga, “The dynamic field of Haskell’s rectangular dislocation fault model”, *Bull. Seismol. Soc. Am.* **68** (1978) 869–887.
- [42] P. K. F. Kuhfittig, *Introduction to the Laplace Transform*, vol. 8 of *Mathematical concepts and methods in science and engineering*, A. Miele, ed., (Springer-Verlag, 1978).
- [43] X. Markenscoff, “The singularities of nonuniformly moving dislocations”, *Int. J. Solids Struct.* **21** (1985) 767–772.
- [44] J. R. Rumble, ed., *CRC Handbook of Chemistry and Physics*, 100th ed., (CRC Press, 2019).
- [45] C. Callias and X. Markenscoff, “The nonuniform motion of a supersonic dislocation”, *Quart. Appl. Math.* **38** (1980) 323–330.
- [46] C. Callias and X. Markenscoff, “Singular asymptotics of integrals and the near-field radiated from nonuniformly moving dislocations”, *Arch. Ration. Mech. Anal.* **102** (1988) 273–285.
- [47] D. N. Blaschke and D. J. Luscher, “Dislocation drag and its influence on precursor decay”, LA-UR-20-25546, in preparation.
- [48] R. A. Austin, “Elastic precursor wave decay in shock-compressed aluminum over a wide range of temperature”, *J. Appl. Phys.* **123** (2018) 035103.
- [49] J. D. Eshelby, “Uniformly moving dislocations”, *Proc. Phys. Soc.* **A62** (1949) 307.
- [50] X. Markenscoff and L. Ni, “The transient motion of a dislocation with a ramp-like core”, *J. Mech. Phys. Solids* **49** (2001) 1603–1619.
- [51] E. Clouet, “Dislocation core field. I. Modeling in anisotropic linear elasticity theory”, *Phys. Rev.* **B84** (2011) 224111, [arXiv:1112.4938 \[cond-mat.mtrl-sci\]](#).
- [52] B. A. Szajewski, A. Hunter, and I. J. Beyerlein, “The core structure and recombination energy of a copper screw dislocation: a Peierls study”, *Phil. Mag.* **97** (2017) 2143–2163.
- [53] M. Boleininger and S. L. Dudarev, “Continuum model for the core of a straight mixed dislocation”, *Phys. Rev. Mater.* **3** (2019) 093801.
- [54] B. Gurrutxaga-Lerma and J. Verschuere, “Generalized Kanzaki force field of extended defects in crystals with applications to the modeling of edge dislocations”, *Phys. Rev. Mater.* **3** (2019) 113801.